Batteries' end of life: Modelling the ageing phenomena

Clément Bernard Guy Lucien LESAGE

Thesis to obtain the Master of Science Degree in

Energy Engineering and Management

Supervisors: Prof. Diogo Miguel Franco dos Santos
Dr. Alain Hita

Examination Committee:

Chairperson: Prof. Duarte de Mesquita e Sousa
Supervisor: Prof. Diogo Miguel Franco dos Santos
Member of the Committee: Dr. Rui Miguel da Silva Sampaio

December 2023

I declare that this document is an original work of my own authorship and that it fulfills all the requirements of the Code of Conduct and Good Practices of the Universidade de Lisboa.

Declaro que o presente documento é um trabalho original da minha autoria e que cumpre todos os requisitos do Código de Conduta e Boas Práticas da Universidade de Lisboa.

Acknowledgements

I would like to first thank Professor Diogo M.F. Santos for his constant presence and availability throughout the execution of this master thesis work. His support and advice were essential and greatly helped me in my subject orientation.

I would also like to thank the EIT InnoEnergy team, both at Instituto Superior Técnico and Politecnico di Torino for their support and guidance.

Finally, I would like to thank my teachers from all disciplines who have transmitted to me the sense of critical thinking and the drive to perform well. I would not be here without them.

Abstract

In the context of a growing deployment of renewable energy capacities, the electric grid faces challenges related to the intermittency of such energy sources. To ensure flexibility, energy storage is necessary. It may involve installing electrochemical batteries linked to the grid, designed to store the electricity overload, and deliver it back when needed. The service life of these batteries is expected to reach 10 years minimum and 20 years, if possible, with on average 1 cycle per day (amounting to 3000 to 8000 cycles). From that perspective, it is necessary to understand the ageing phenomena leading to battery end-of-life. Modeling those allows for accurate forecasts of the battery's behavior throughout its lifetime. For many lithium-ion systems, recent studies have shown that ageing happens in three phases, with first, the formation of the SEI layer at the anode which provokes a first drop in capacity. The second phase consists in a linear decrease of the battery capacity due to the growing of the SEI phase at the anode side. The third phase often referred to as knee-point consists in the sudden and drastic drop in capacity primarily due to the deposition of metallic lithium onto the anode material. The aim of this Master Thesis is to present an overview of the different ageing mechanisms taking place in a lithium-ion battery and the attempts to model them, with a focus on the SEI/lithium-plating combination.

Keywords: Lithium-ion battery, Ageing, Simulation, Lithium-plating, Knee-point

Resumo

No contexto de uma implantação crescente de energias renováveis, a rede eléctrica enfrenta desafios relacionados com a intermitência dessas fontes de energia. Para garantir a flexibilidade, é necessário o armazenamento de energia. Pode envolver a instalação de baterias electroquímicas ligadas à rede, concebidas para armazenar a sobrecarga de eletricidade e devolvê-la quando necessário. Prevê-se que a vida útil destas baterias atinja, no mínimo, 10 anos e, se possível, 20 anos, com uma média de 1 ciclo por dia (o que equivale a 3000 a 8000 ciclos). Nesta perspetiva, é necessário compreender os fenómenos de envelhecimento que conduzem ao fim da vida útil das baterias. A modelação destes fenómenos permite fazer previsões precisas do comportamento da bateria ao longo da sua vida útil. Para muitos sistemas de iões de lítio, estudos recentes mostraram que o envelhecimento se processa em três fases, sendo a primeira a formação da camada SEI no ânodo, que provoca uma primeira queda na capacidade. A segunda fase consiste numa diminuição linear da capacidade da bateria devido ao crescimento da fase SEI no lado do ânodo. A terceira fase, muitas vezes referida como *knee-point*, consiste na queda súbita e drástica da capacidade, principalmente devido à deposição de lítio metálico no material do ânodo. O objetivo desta tese de mestrado é apresentar uma visão geral dos diferentes mecanismos de envelhecimento que ocorrem numa bateria de iões de lítio e as tentativas de os modelar, com um enfoque na combinação SEI/lítio revestido.

Palavras-chave: Bateria de iões de lítio, Envelhecimento, Simulação, Revestimento de lítio, Ponto de joelho

Index

I. Electrochemical devices 7
1) Lithium-ion batteries fundamentals 8
1.1) Introduction to lithium-ion batteries 8
a. Working principle of Li-ion accumulators 10
b. Important definitions: State-of-Health (SoH) 11
c. Important definitions: State-of-Charge (SoC) 11
i. Electrodes 11
ii. Battery 11
1.2) Materials involved in lithium-ion batteries 12
a. Focus on the positive electrode 12
b. Focus on the negative electrode 13
i. Solid Electrolyte Interface (SEI) 14
c. Electrolytes 15
II. Battery ageing and modelling 16
Gr/LFP case study 16
1) Ageing and modelling interest 17
1.1) Ageing 17
a. Battery ageing: at the battery scale 17
i. Calendar ageing 17
ii. Ageing in cycling 18
i. Negative electrode main ageing mechanisms 19
ii. Positive electrode main ageing mechanisms 20
c. Ageing profiles 21
d. Lithium-plating 23
1.2) Modelling 25
a. Interest for simulation 25
b. Battery models 26
ii. P2D model 27
iii. Empirical models 27
iv. Single-Particle Model 27
v. Global Battery modeling 28
III. Mathematical model 28
1) Introduction to the model and simulation 28
2) Newman's model 29
a. Porous electrode theory 30
b. Current densities and reactions 31

c. Ageing implementation 31
i. SEI layer 31
ii. Lithium plating 33
3) Model input 33
a. Geometrical attributes 33
b. Electrode composition 33
i. Porosity-Volume fractions 33
ii. Active sites concentration 34
iii. Electrode balancing 34
iii.1. Anode/Cathode ratio (N/P ratio) 35
iii.2. Shift of operational window 35
iv. Time accelerating factor 38
v. Battery operation parameters 38
4) Exploitation of experimental data 38
a. Cycling trials data 38
b. SEI layer formation and growth simulation 39
c. Lithium plating and superlinear degradation 41

Figures

Figure 1: General structure of a lithium-ion battery 9
Figure 2: LFP Olivine structure 12
Figure 3: Schematic diagram showing intercalated lithium between graphite planes 13
Figure 4: Capacity loss for a Gr/LMO cell with varying storage time (up to 5 years) and temperature [17] 18
Figure 5: Potential and specific capacity of active materials in Li-ion batteries [20] 19
Figure 6: Main degradation mechanisms in Li-ion cells [22] 20
Figure 7: Schematic of three lithium-ion ageing trajectories, sublinear, linear and superlinear degradation (“knee”). The x-axis represents the cycle numbers. The y-axis “Retention” can represent capacity, power retention. [24] 21
Figure 8: Battery capacity fade with possible mechanisms in different stages [26]……. 22
Figure 9: Capacity retention(%) evolution for the Gr/LFP cell upon cycling…… 22
Figure 10: Schematic of lithium-plating/stripping at the graphite anode [27]…….. 23
Figure 11: Ideal conditions, no lithium plating [27]…….. 23
Figure 12: Lithium plating occurence at low-temperature, accumulation of lithium ions at the graphite/electrolyte interface [27]……...243
Figure 13: Lithium plating occurence at high charging C-rate, too many lithium ions are arriving to intercalate and are blocked by the solid diffusion limitations [27]……..24
Figure 14: Lithium plating occurence at high SoC [27] 24
Figure 15: Simulation types depending on the space length and time period they are used to simulate events in [28] 25
Figure 16: Representation of different battery models with respect to their complexity and accuracy 26
Figure 17: Simplified scheme of the cell with the x-axis coordinates and the different cell components 28
Figure 18 : Subdomains on Comsol Multiphysics 29
Figure 19 : Equilibrium potential evolution for Graphite anode versus SoC 35
Figure 20 : Equilibrium potential evolution for LFP cathode versus SoC 36
Figure 21: Illustration of the effect of first cycles on the electrodes potential window in the assembled cell [45] 3737
Figure 22: Initial cell charge distribution COMSOL section 3737
Figure 23: Gr/LFP cell ageing profile, showing capacity retention through cycling…….. 39
Figure 24: Linear degradation part, with linear regression……... 39
Figure 25: Capacity retention evolution in COMSOL for the SEI layer……... 40
Figure 26: Comsol capacity fade with corrected SEI current density……. 40
Figure 27: Knee-point phenomenon observed for the Gr/LFP cell…….. 41
Figure 28: Electrolyte volume fraction evolution versus the number of cycles…….. 41

I. Electrochemical devices

1) Lithium-ion batteries fundamentals

1.1) Introduction to lithium-ion batteries

The first appearance of rechargeable Li-ion secondary batteries took place in 1990, and from then on, the capacity always increased in response to the always more demanding energy market. [1] The corresponding cells can contain either liquid electrolytes or polymer electrolytes, with a wide range of anode and cathode materials which allow for a fine tuning of the batteries' performance. Ideally, these devices are the best fit for having the greatest energy content than their counterparts.

Advantages of lithium-ion batteries are numerous, notably if put in regard with other types of accumulators [2].

- High cell voltage: the working voltage can range from 1.5V up to 4V and beyond.
- High specific energy: ranges from 80 to 300 $Wh.kg^{-1}$, depending on the cell type and the materials involved
- High energy density: from 250 to 1000 $Wh.l^{-1}$
- Stability during charging phase: the potential obtained during the charging phase reaches a good stability level which is convenient while considering the use of electronic devices.
- Low capacity losses, with respect to other battery types

These advantages come with some disadvantages. Lithium-ion batteries can be costly, due to the volatility of lithium price and the sometimes expensive manufacturing of electrode materials. Compared with past years, the cost was reduced thanks to production scaling-up by gigafactories and incremental improvements on the process and performances. Other important points are the safety when in use, the thermodynamic conditions and the temperature of use. The temperature in particular must be closely monitored as fire hazard can be present. Figure 1 gives a schematic of the general structure of a lithium-ion battery.

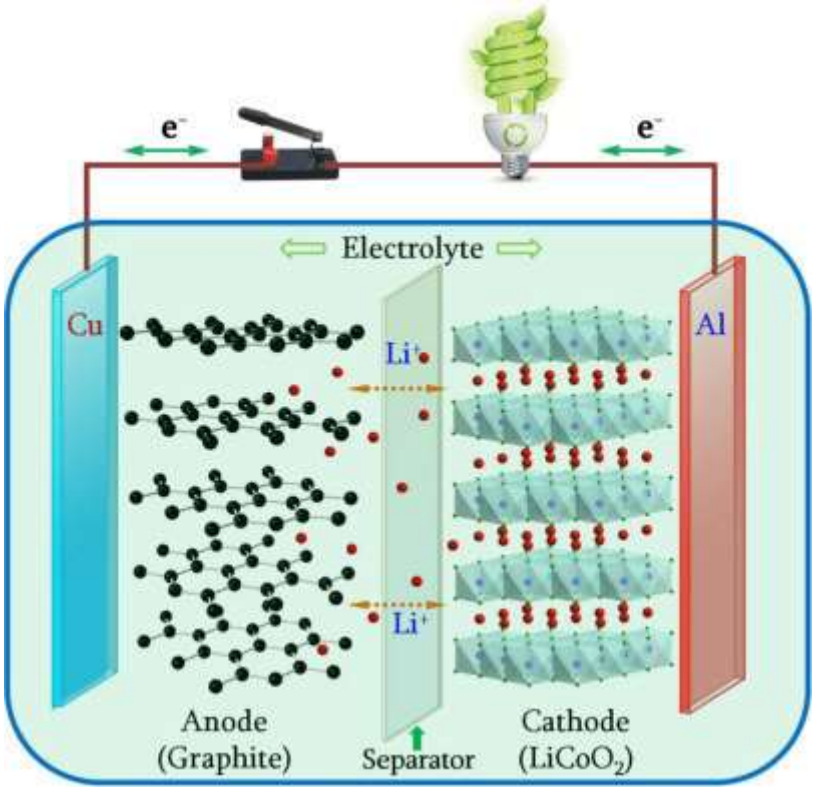

Figure 1: General structure of a lithium-ion battery [3]

In case of overcharge or overheating, lithium-ion cells can be subject to explosions or fires. These risks, in order to be mitigated, require the implementation of several security measures, such as pressure sensors, or thermal interrupters. In general, these issues can be directly linked to the cells' materials.

In classical Li-ion batteries, anodes are generally made out of carbon material such as graphite, which shows a potential close to 0 V vs. Li/Li^+(0.02 V when fully lithiated). It follows that the energy properties of the cell, such as energy density and specific power are conditioned by the choice of the cathode material.[3] During the choice of an adequate cathode material, manufacturers have often tried to target materials allowing for high current usage and a larger potential window to reach 5V, as to obtain a larger power output. The widening of the cell's working voltage window is a feature vastly researched, but that favors the instability of the electrolyte. The cells operating at high current/voltage regimes necessitate the use of electrolyte solvents with sufficient chemical and electrochemical stability so as to avoid further degradation reactions.

For example, most electrolytes used today are flammable and unstable at high potential (around 4.5 V). As a result, liquids made up of a solvent with a lithium salt are chosen as electrolytes, but those are responsible for the formation of the "Solid Electrolyte Interface" (SEI), a solid layer made of components derived from the reaction taking place between the electrolyte molecules and the active material particles. This layer is fundamental to prevent carbon delamination phenomena. The SEI layer is also essential for the stability of graphite.[4] Another alternative for the electrolyte resides in using ceramic electrolytes, presenting a high ionic conductivity. However those are still in research phase and are not yet commercialized.

a. Working principle of Li-ion accumulators

The total reaction taking place in a classic Li-ion accumulator with a graphite anode is given in Eq. 1:

$$C_6Li_x + Li_{1-x}MO_2 \Leftrightarrow 6C + LiMO_2 \quad (1)$$

where the M represents a metal. There is a Li ions exchange between the two active materials. This equation is defined for the discharge process. The complete reaction comes from the two half-equations coming from the oxidation (Eq. 2) and reduction (Eq. 3) taking place, which have the following form during the discharging phase:

$$C_6Li_x \Rightarrow 6C + xLi + xe^- \quad (anode) \quad (2)$$

$$Li_{1-x}MO_2 + xLi^+ + xe^- \Rightarrow LiMO_2 \quad (cathode) \quad (3)$$

Being present in several equations, the choice of M is quite important from a thermodynamics perspective, as it helps to determine the total ΔG (Gibbs free energy) of the reaction, and therefore also contributes to determine the cell open-Circuit Voltage (OCV) and other related parameters.

The quantity x represents not only a stoichiometric coefficient, but also indicates the number of sites where can be intercalated the lithium in the electrode. The intercalation is a very important part of the lithium ions diffusion process. During the discharge, ions de-intercalate from the anode structure (they abandon a site where lithium was connected to a graphite plane) and flow through the anode, then the electrolyte and then the cathode.

Similarly, the electrons abandon the sites where they were linked to a lithium ion, propagate through the current collectors (and not the electrolyte), flow through the external conductor (sometimes linked to an outside user) and then recombine with Li ions at the cathode. In this last step, the intercalation process also takes place. Usually, the electrodes showcase a porous structure in order to favor the intercalation process. The intercalation presents three major steps:

1) Diffusion of Li ions in the electrolytic solution
2) Fading of the electrolyte-ions bonds and start for the ions to go to the electrode material vacant sites
3) Diffusion of Li ions inside the active material structure

As all diffusivity-linked phenomena, intercalation is a dynamic process, which means that different graphite layers are reached with different times. This induces a substantial raise in the ions' path length inside the active material, thus impacting the polarization and the overpotentials.

b. Important definitions: State-of-Health (SoH)

A battery starts off with a nominal capacity, usually provided by the manufacturer. This nominal capacity depends on the battery chemistry, the type of materials involved. The State-of-Health is a metric measuring the ageing level of a battery. It often includes capacity or power fade. [5]

In this study the battery's State-of-Health (SoH) is defined in Eq. 4:

$$SoH = \frac{Q_t^{max}}{Q_0^{max}} \quad (4)$$

where, Q_0^{max} designates the battery maximum capacity at the beginning of its life, and Q_t^{max} represents the battery maximum capacity at time *t*. Given the fact that battery age, the SoH is bound to decrease throughout the battery's lifetime.

c. Important definitions: State-of-Charge (SoC)

The definition of the State of Charge (SoC) will be presented at electrode level and battery level.

i. Electrodes

Most of lithium-ion batteries follow a "rocking-chair" principle where lithium ions travel back and forth between the electrodes and through the separator in the electrolyte. Often also, lithium-ion batteries rely on intercalation/deintercalation mechanisms within their electrode materials to ensure that rocking-chair scheme for lithium ions.

Like sugar and salt in water, lithium can only be present in a certain amount within a host material structure. Therefore, one of the electrode materials characteristics is the maximum quantity of lithium that they can host in their structure. This is described by the reference equilibrium concentration which shows the maximum number in moles of host sites for lithium atoms per cubic meters of electrode active material.

Therefore, talking about the SoC of an electrode designates the amount of cyclable lithium contained in the electrode at a given moment in time (Eq. 5).

And so,

$$SoC = \frac{c_s}{c_{s,max}} \quad (5)$$

where c_s is the electrode current lithium concentration, while $c_{s,max}$ is the maximum achievable lithium concentration for the studied electrode, both expressed in $mol.m^{-3}$.

ii. Battery

A battery possesses a maximum capacity referred to as Q_{max} often expressed in Ah. Often, batteries do not undergo complete discharge, where the remaining available energy would be equal to zero. On many mobile devices, a battery State-of-Charge (SoC) indicator is shown indicating the percentage of charged battery. This Soc is defined in Eq. 6:

$$SoC = \frac{Q_t}{Q_{max}} \quad (6)$$

where, Q_t is the battery's charge at instant *t*. This SoC refers to the available capacity in the battery compared to the maximum attainable one.

1.2) Materials involved in lithium-ion batteries

The cell's intrinsic properties are linked to the materials, whichever battery technology is used. Among them, the effective cell life, as well as the cyclability. (It is important to note that, though the cell's materials are important, battery's lifetime is also influenced by the choice of electrolyte, the cell assembly process, the size of the electrode particles, the choice of coating, etc…). To the present day, lithium-ions accumulators have been extensively researched and studied. The choice and study of a material depends a lot on the required power, but also on the material availability. For example, a screening feature for the choice of material can be the working voltage, which would involve a low working potential battery for pure electronic applications or a high working potential battery such as the lithium-ions ones. Added to this one, many more considerations come into play, such as the safety and reliability concerns. Below, figures a quick description of the involved materials in the studied cell, a Graphite/LFP one.

a. Focus on the positive electrode

This material, which full formula is $LiFePO_4$, is quite popular, cheaper than other technologies and widely used, for example, in electromobility [6]. Polyanionic compounds such as LFP present molecules of the $(XO_4)^{3-}$, with X representing one of the following metals, Silicon, Phosphor, Arsenic, Molybdenum or Tungsten. These compounds occupy specific positions in the crystalline network, allowing for a structural stability increase, as well as an increase in the oxidoreduction potential. However, they often showcase a limited electronic conductivity which brings the necessity for additional treatments to make them efficient.

LFP presents an olivine structure (Fig. 2), showcases a good thermal stability and allows to reach a high delivery power. However, this material works at low potentials, with low ionic and electric conductivity.

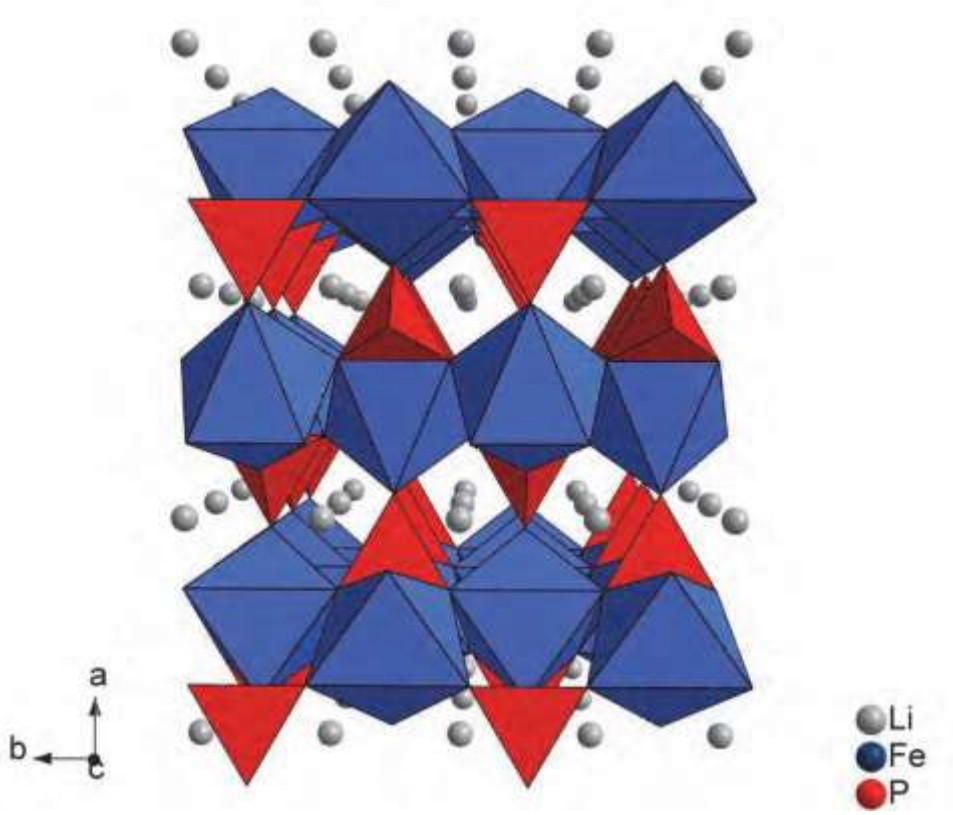

Figure 2: LFP Olivine structure [6]

Several studies [5,6] have been conducted to improve this material and attempts have been made, such as realizing micro-particles of this material combined with a carbon binder and a cationic doping. Several improvements have been reported for different C-rates. At times, good performances can be obtained without the carbon binder, just with uniform nanoparticles associated with carbon nanoparticles (conductive) inside the cathode. The ionic conductivity issue has been recently tackled and research has been conducted to determine the best additives to improve that specific property.

b. Focus on the negative electrode

For anodes, the currently most used material is graphite. Research on this material have allowed for always more efficient products. The theoretical specific capacity of graphite is $372\ mAh.g^{-1}$.[7]

Lithium intercalation happens between the planes constituting graphite (Fig. 3). These planes are bonded between them through medium to low energy Van der Waals interactions. This disposition, determines the material's characteristics:

1) Mechanic stability of the planes
2) Good electric conductivity
3) Optimal ionic transport of Li^+

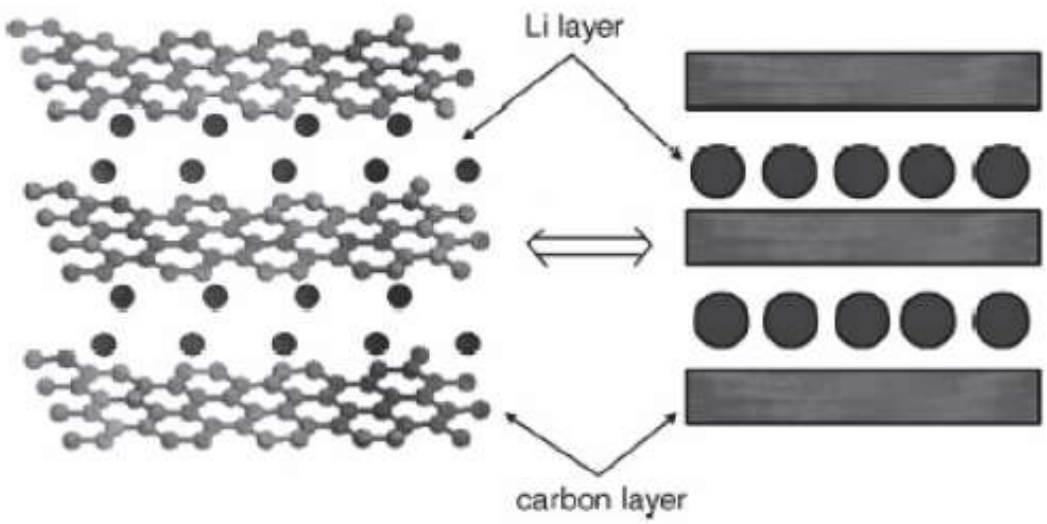

Figure 3: Schematic diagram showing intercalated lithium between graphite planes [7]

To these physico-chemical properties related to the nature of the material, others, of different nature, are present:

1) Low potential required for delithiation
2) Optimal lithium diffusivity
3) Low volume variation rate during intercalation and de-intercalation of lithium
4) Low cost
5) Abundant material

The major disadvantages of this material is its reactivity and the interactions it can have with different types of electrolytes, in particular those based on carbon such as the widely used propylene carbonate (PC). The PC molecules tend to insert between the planes with the lithium ions, causing the graphite to exfoliate and leading to a capacity decrease. This phenomenon does not take part in SEI formation but given the fact that it severely stresses the graphite structure, it can damage the SEI and further reduce the battery life. All these issues have, nonetheless, not led to a replacement for graphite as the anode material. It is crucial to highlight the importance of the SEI layer, as it is formed during the battery's early cycle uses and then continuously grows throughout its lifetime. As an important reaction taken into account in this study, a description of the SEI layer is provided in the following part.

i. Solid Electrolyte Interface (SEI)

The SEI is primarily responsible for the capacity loss in lithium-ion batteries, particularly due to the intercalation of lithium ions inside the capacitive layer [9]. During the first cycles, the SEI protects the electrode from additional decomposition reactions with electrolyte molecules and allows the passage of lithium ions to the active material and back to the electrolyte.

The SEI forms after the irreversible decomposition reaction of the electrolyte due to the application of an external current, known as "faradic current". Faradic current is related to the electrode's oxidation reaction. This current is qualified as "faradic" because it is defined through Faraday's law (Eq. 7):

$$I_{Farad} = nFAv \quad (7)$$

where n is the number of moles, F is the Faraday constant, A is the electrode's area and v is the concentration variation rate with time (expressed in $mol.s^{-1}$)[10].

These decomposition reactions take place spontaneously due to the electrolyte's instability during the charging phase because its potential is outside of its own stability window. During the first charging phases of the cell, the capacity irreversibly fades due to the formation of the initial SEI layer [11].

Once stabilized, the SEI layer is not able to be electronically conductive and this explains why it is not directly responsible for a possible battery failure. Furthermore, this layer is impermeable to electrolyte molecules. This way, no other electrolyte molecules can come in contact with the electrode active material, creating more SEI. Therefore, the SEI layer remains stable and does not impede the cell to properly function but also increases the anode material stability and cyclability (taking, for example, graphite). The SEI layer is essential for the cell's stability.

However, the structural integrity of the anode material, such as graphite, can be subjected to mechanical stress due to intercalation and de-intercalation, leading to cracking [15]. Depending on the cracking speed, negative consequences can arise: if the cracking is fast, the electrolyte will flow through it and react with the active material to create new SEI and expand it; if the cracking is slow, the anode slowly expands, and the SEI layer's thickness decreases. This reduction can provoke unwanted reactions between the electrons and the electrolyte molecules. Both processes are retroactive under a crack/reparation form.

c. Electrolytes

The electrolyte is the third component of a battery, with the role to separate the reactions taking place at the electrodes to guarantee the energy output and close the cell's circuit. This means stabilize the anode and cathode's energy levels during the cell's operation [5]. The electrolyte presents itself in the form of a solution constituted of a solvent (organic or inorganic) and a salt (generally a lithium salt). The choice of the material is crucial, as several parameters are dependent on it: energy density, charge/discharge kinetics, stability, safety, and reliability of the cell. [16]

In order to be chosen for a cell, an electrolyte solution must abide by some pre-requisite:

1) Divide the ions and electrons path, making sure that electrons do not get carried by the electrolyte molecules
2) Ease the transport of ions (lithium, for example)
3) Be able to penetrate the electrode and separator porous material
4) Be easily stored, not subjected to leakages
5) Be resistant to possible undesired reactions with the electrode's active material
6) Ensure the cell's electrochemical activity within the potential window

II. Battery ageing and modelling
Gr/LFP case study

1) Ageing and modelling interest

In this part, a definition of battery ageing will be given. First of all, different ageing types, as well as different ageing observable features will be described. The main ageing mechanisms will be presented, with respect to the electrode type. Lithium plating, subject of interest for this work will be presented as well. Then, a brief history of simulation and its interest in the field of batteries will be given. Finally, different digital battery models will be described.

1.1) Ageing

In this “Ageing” part, first will be presented its meaning at the battery scale. Then its manifestation at the material scale will be discussed, focusing on the electrode material. Different ageing profiles will be showed and the “Ageing” part will finish with the presentation of the lithium plating phenomenon.

a. Battery ageing: at the battery scale

As batteries are used, different side reactions can take place, such as the previously mentioned SEI formation and growth. These side, or “parasitic” reactions can worsen the performance of the batteries and are observed throughout the whole lifetime of a battery. Overall, these reactions are responsible for the capacity fade of a battery and are therefore responsible for the ”ageing” of the battery.

One can distinguish two types of ageing for batteries. The first type of ageing for batteries is referred to as calendar ageing, which takes place when the battery is not being used. In the automotive industry, it is referred to as “parking mode”. One must beware not to confuse this ageing type, which induces an irreversible capacity loss, with the self-discharge phenomenon, which only provokes a reversible loss of capacity.

The second ageing type for batteries is called ageing in use or in cycling, which takes place when the battery is used either in charge or discharge mode.

i. Calendar ageing

Calendar ageing (Fig. 4) is the term used for ageing taking place while the battery is being stored, not being subject to any charge/discharge cycles. It translates into irreversible capacity loss. This battery degradation mode mainly depends on two factors, which are the storage temperature and the battery’s SoC.

The higher the storage temperature, the faster calendar ageing happens. Similarly, calendar ageing will be important for a battery at a high SoC rather than for one with presenting a low SoC. Usually, a battery manufacturer will indicate a temperature range for storage, depending on the Li-ion technologies and electrode materials involved. Though provided by the manufacturer, the upper limits of the temperature range can sometimes lead to significant calendar ageing.

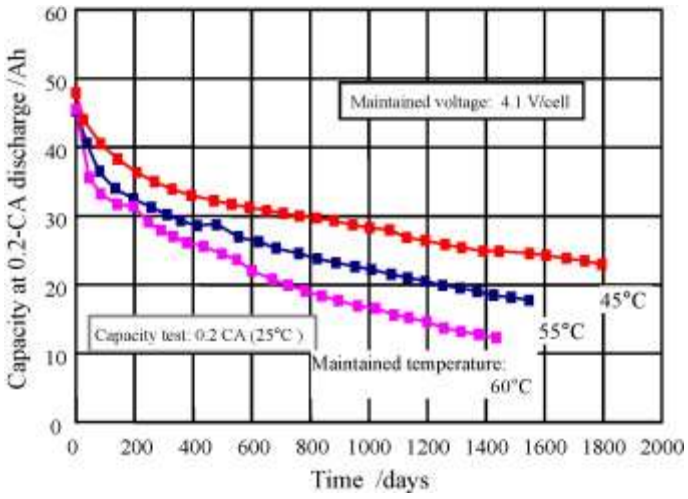

Figure 4: Capacity loss for a Gr/LMO cell with varying storage time (up to 5 years) and temperature [14]

As seen in Figure 4, calendar ageing is an important parameter to take into account for mobile devices, as several devices can stay stored for long periods of time without being used (such as electric vehicles). In this study, a focus will be made on ageing in cycling, as the envisioned application is for stationary storage.

ii. Ageing in cycling

Ageing in cycling takes place when the battery is used through several charge/discharge cycles. Ageing causes are more complex and with more contributions than for calendar ageing. It has been acknowledged that the battery's working temperature, the SOC variation range, the maximum current value for charge and discharge, the average current applied on a time interval and the current profile, count among the parameters influencing the ageing in cycling.

b. Battery ageing: at the material scale, internal parameters and phenomena

Overall, degradation in lithium-ion batteries is caused by a variety of reactions, involving one or more battery components, among which the electrolyte, the electrodes, the current collectors and the separator. Many degradation phenomena affect those different components, and these phenomena are sometimes inter-dependent. Simulating all of these phenomena becomes quite challenging when considering commonly available computing resources, and this is why a majority of physics-based models only take into account the dominant mechanisms, like the formation and growth of the SEI [9] or the loss of electronic contact through cracking [15].

i. Negative electrode main ageing mechanisms

Most lithium-ion accumulators contain graphite as the anode material. However, as shown by Figure 5, the electrochemical stability voltage window of conventional liquid electrolytes ranges from 1V to 4.5V [16], while graphite presents a working voltage of about 0.05V. This value is outside of the electrolyte stabilized voltage window, thus making the system based on graphite unstable (Figure 5).

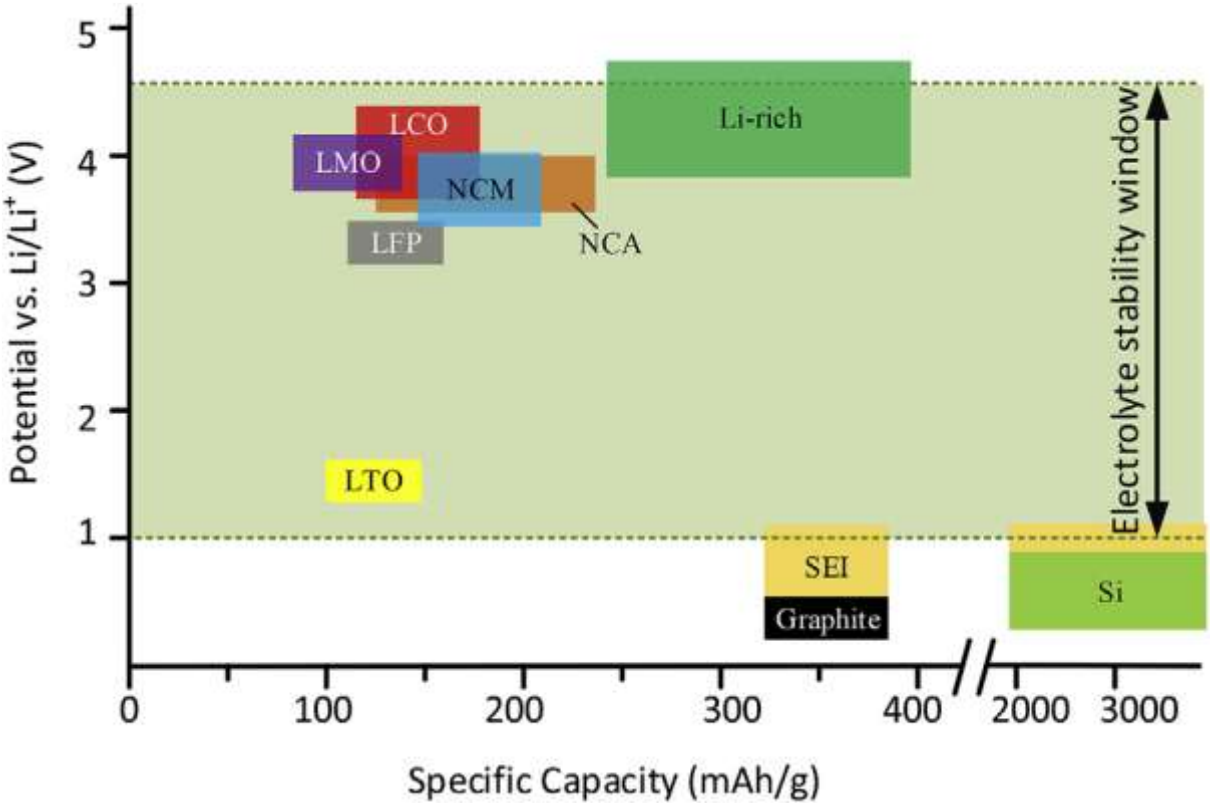

Figure 5: Potential and specific capacity of active materials in Li-ion batteries [17]

However, the graphite-based technology is viable due to the fact that the electrolyte decomposition product, coming from a reaction with graphite, form a passivation layer, the SEI. This layer is permeable to lithium ions, therefore allowing the intercalation/deintercalation of lithium ions. It is however impermeable to electrolyte molecules and electrons.

The SEI layer, though allowing for the existence of graphite-based lithium-ion batteries, is also considered to be the main cause of ageing. Indeed its passivation property is never perfect, and SEI keeps on being created throughout the battery's life, leading to unbalance in the battery and provoking a constant loss of cyclable lithium, therefore decreasing the battery's global capacity. The SEI increase also leads to an increase in the battery internal resistance.

Other degradation mechanisms can take place. For example, the lithium metal deposition taking place either at low temperature charging, high C-rate charging or overcharging can also contribute to the loss of cyclable lithium and ultimately to global capacity loss. [18]

Sometimes, co-intercalation of lithium ions with solvent molecules of the electrolyte can lead to graphite particles exfoliation (separation of graphite layers) creating “dead zones” in the electrode and therefore causing the loss of active material. Furthermore, current collectors corrosion and binder decomposition can provoke loss of active material as well. [17] Different degradation mechanisms are presented Figure 6.

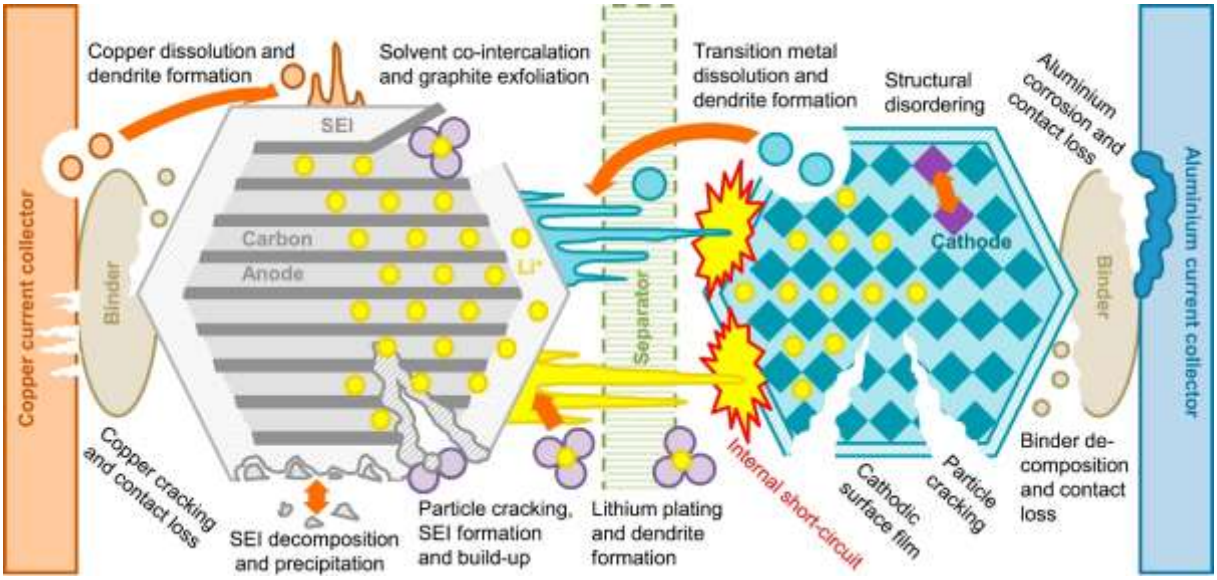

Figure 6: Main degradation mechanisms in Li-ion cells [19]

ii. Positive electrode main ageing mechanisms

Similarly, to the negative electrode, ageing for positive electrode can come from the active material itself (dissolution, phase transition, amorphization, etc…) or from the whole electrode taking into account all of its components (binder degradation, current collectors corrosion, electrode decohesion, etc.). The parasitic oxidation reactions of the electrolyte at the electrode surface are often encountered at high state of charge and high temperature. As for the reactions taking place at the negative electrode, these ones also cause unbalance within the battery. These reactions are, however, less documented than the negative electrode degradation reactions. The degradation reactions product can be solid, so as to form a passivation layer similar to the SEI, called the cathode electrolyte interface (CEI), but can also be gaseous or soluble in the electrolyte. In this last category are protons, particularly harmful as they can react with PF_6^- to form HF, known to react with the SEI at the negative electrode side.

A widespread cathode material, and the one subject of the present study, is referred to as LFP. LFP stands for lithium iron phosphate, of chemical formula $LiFePO_4$. This cathode material is one of the best compromise between cost and performance. As a matter of fact, LFP cathode show low voltage and high resistance, which means that the energy density is lower than the average.

In terms of degradation, LFP does not present much well-documented phenomena. At least, the iron ions can undergo dissolution in the electrolyte and flow to the anode, where they react with the SEI layer, causing an increase in internal resistance and consuming cyclable lithium causing more loss of lithium inventory. [20]

c. Ageing profiles

One of the main manifestations of the ageing phenomena for lithium-ion batteries is the capacity loss. From tests, such as calendar ageing or charge/discharge cycles, the battery capacity can be extracted and represented function of time or function of the number of cycles.

Ageing profiles, or ageing trajectories can come in many shapes, respectively as sublinear degradation, linear degradation or superlinear degradation, as shown in Figure 7.

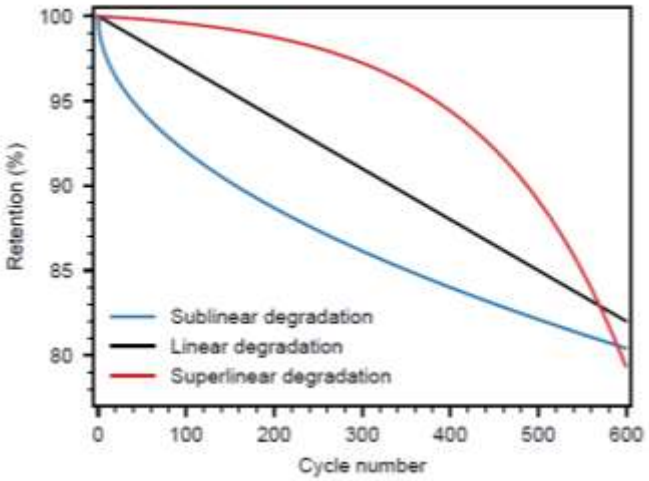

Figure 7: Schematic of three lithium-ion ageing trajectories, sublinear, linear and superlinear degradation ("knee"). The x-axis represents the cycle numbers. The y-axis "Retention" can represent capacity, power retention [21].

Sublinear degradation is often linked to the formation and growth of the SEI layer. As previously mentioned, this type of degradation cannot be avoided, but allows for the battery stability and allows long-term battery application. Added to that, superlinear battery degradation is also commonly observed. This superlinear behavior is referred to as "knee" or "rollover failure"[22]. The terms "knee" or "knee-point" (KP) will be used throughout this report.

As knees provoke a sharp drop in capacity retention, forecasting them is of paramount importance to ensure long battery lifetimes or at least battery optimal use. Forecasting also becomes critical when comparing two batteries with identical state-of-health as both could evolve in very different capacity retention directions, depending on the knee's appearance in time. Different pathways leading to superlinear degradation behavior are envisioned by researchers [21], although only one will be of interest in the present work.

One of the pathways leading to a superlinear degradation trajectory in lithium-ion batteries seems to be the appearance of lithium-plating. Figure 8 proposes an interpretation in terms of mechanisms of a commonly observed ageing profile for lithium-ion batteries.

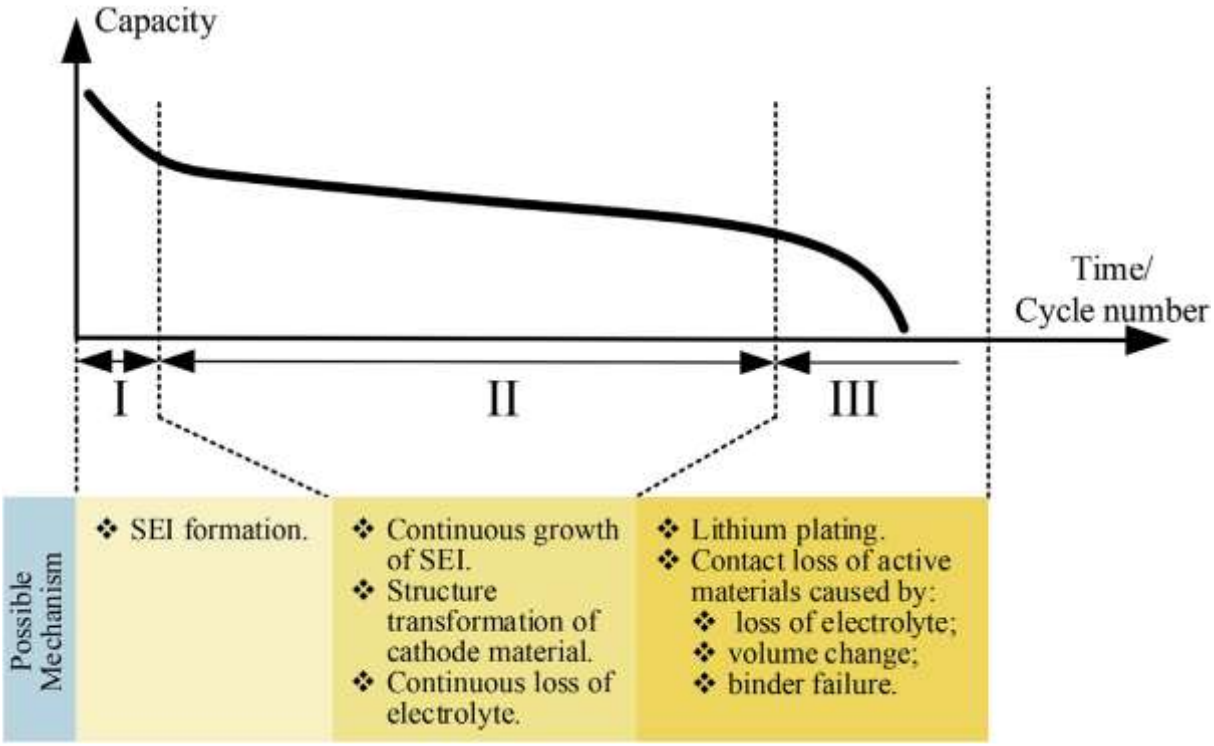

Figure 8: Battery capacity fade with possible mechanisms in different stages [23]

This curve gotten from literature, is similar to what can be obtained experimentally in Figure 9.

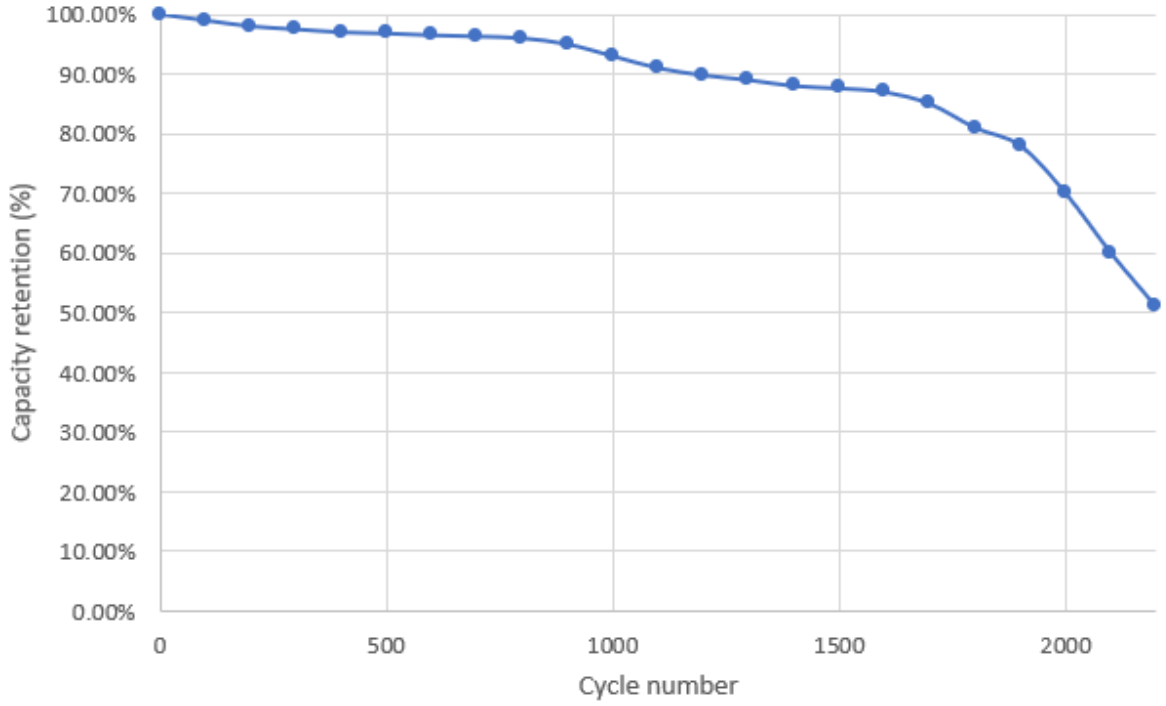

Figure 9: Capacity retention (%) evolution for the Gr/LFP cell upon cycling

d. Lithium-plating

Lithium plating consists in the deposition, under certain conditions, of lithium metal on the surface of an electrode, most commonly the anode, and in the thesis project, on the graphite anode. It happens in preference of lithium intercalation. Graphite, although excellent anode material, is considered vulnerable to lithium plating as its potential is close to the $Li^+/Li(s)$ one.

This metallic lithium deposition can happen under several conditions. Figure 10 shows the different forms that deposited lithium can take. If Figure 11 represents ideal conditions with no lithium deposition, Figure 12 represents a low-temperature situation where lithium metal deposition occurs, as the surface kinetics is slowed down and lithium ions accumulate at the solid-liquid interface. The same phenomenon is observed at high charging C-rate, Figure 13, where the transport of lithium ions in the electrolyte goes much faster than the solid diffusion. Similarly Figure 14, at high SoC, mainly hosting sites are occupied and therefore the diffusion of lithium ions through the lattice is harder causing accumulation at the solid-liquid interface.

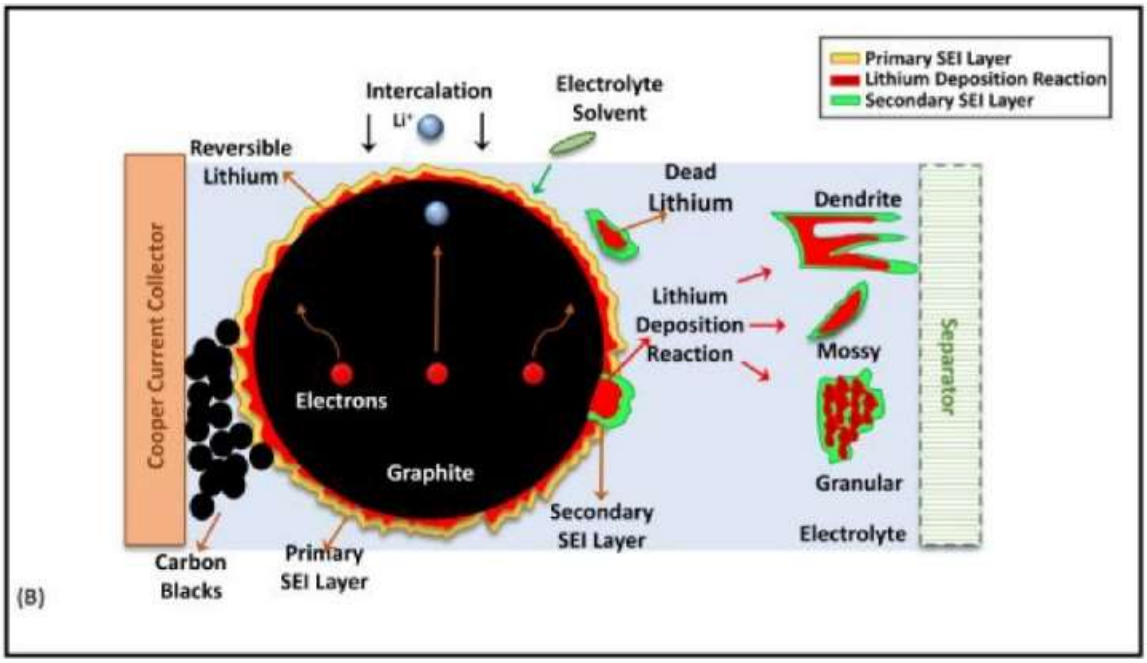

Figure 10: Schematic of lithium-plating/stripping at the graphite anode [24]

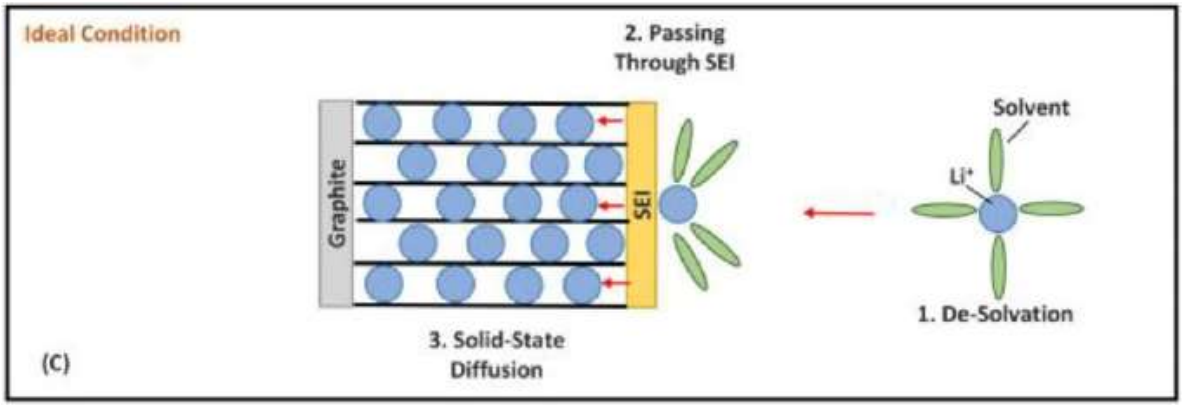

Figure 11: Ideal conditions, no lithium plating [24]

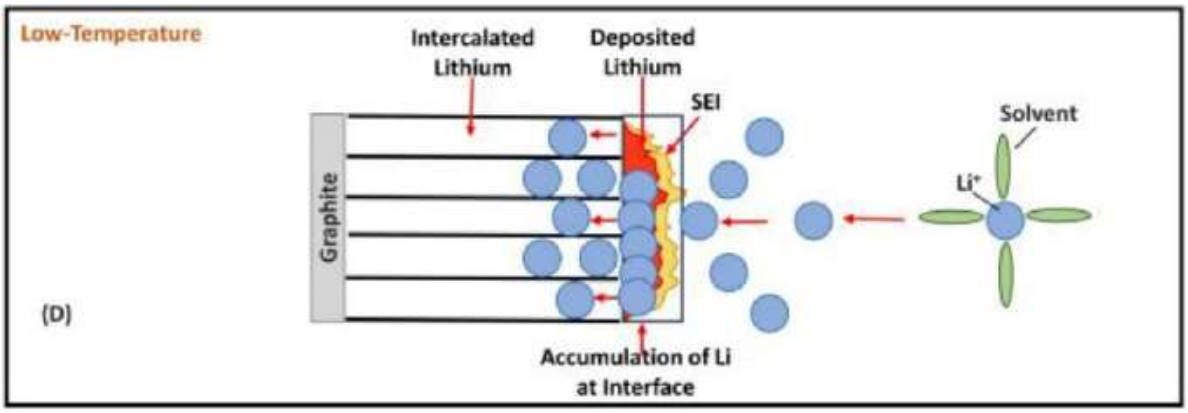

Figure 12: Lithium plating occurrence at low-temperature, accumulation of lithium ions at the graphite/electrolyte interface [24]

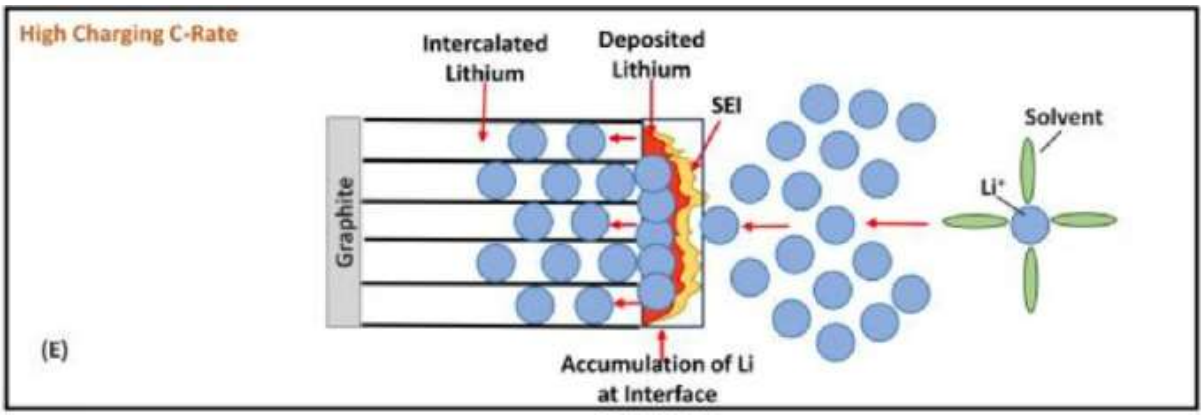

Figure 13: Lithium plating occurrence at high charging C-rate, too many lithium ions are arriving to intercalate and are blocked by the solid diffusion limitations [24]

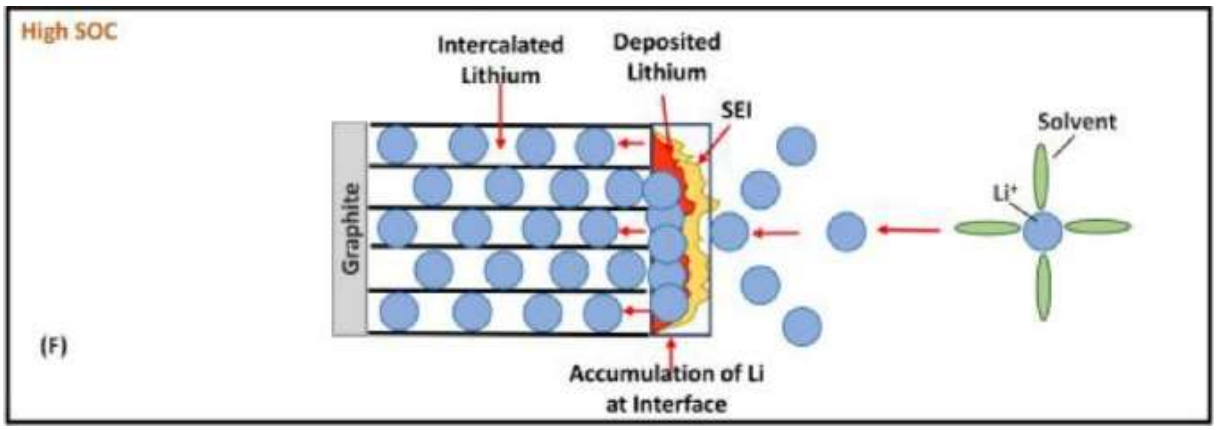

Figure 14: Lithium plating occurrence at high SoC [24]

To fully capture the ageing profile of a lithium-ion battery, one must therefore be able to combine linear degradation and superlinear degradation. Given the interdependent nature of lithium-ion batteries ageing phenomena, a choice must be made on which phenomena to study on a theoretical and modelling perspective. In the present work, the contribution of the SEI layer to cell ageing is associated with the linear degradation phase and the contribution of lithium plating is associated with the superlinear degradation phase.

1.2) Modelling

As dynamic systems, batteries get used and age, due to different physico-chemical mechanisms. Frequent use might sometimes lead them to show some unwanted features for a specific application. If lithium-ion batteries were born in 1990, battery simulation started just after, enhanced later by the explosion of the Internet and the accumulation of data obtained from running battery modules.

a. Interest for simulation

Simulation serves different purposes. Simulation can be done on multiple scales, depending on the type of phenomena to be simulated. (Figure 15)

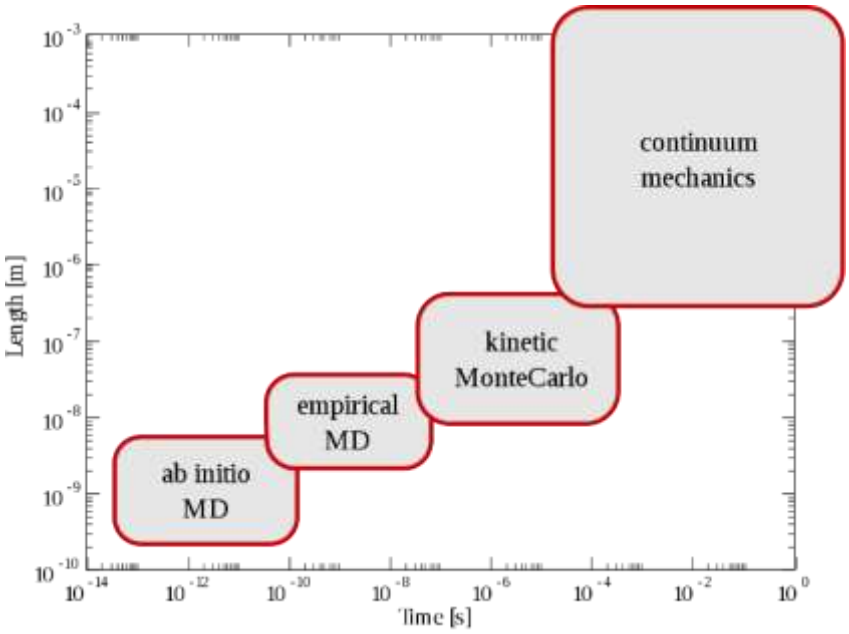

Figure 15: Simulation types depending on the space length and time period they are used to simulate events in [25]

While physical or chemical transformation can be accurately described by a set of equations and boundary conditions in a given situation, many real-life events showcase multiple reactions happening at the same time. This means that most phenomena can happen at the same time, be correlated, cause one another or more globally influence each other. While some equations can be simple, a lot of them makes it a lot harder to compute by hand. Furthermore, simulation is often required to be done over a large period of time, to get a good overview of a system's behavior over time. The interest in simulation comes from the United States. Indeed, after the 1996 Comprehensive Test Ban Treaty, with which several countries pledged to put a halt to all systems-level nuclear testing, programs like the Advanced Strategic Computing Initiative (ASCI) were created within the Department of Energy (DOE) of the United States. This prompted the development of multiscale modeling and simulation-based design. While the shift operated simultaneously across different National Research laboratories throughout the world, industry saw an interest, as such tools could be applied independently from the product type.

Simulation, compared to all-systems level experiments, provides significant budget savings as expensive equipment does not become needed to carry out a full scale study of a component. [25]

For this motive, and with the rapid development of energy storage solutions, modelling and simulation provide an efficient way to understand, design, size and scale complex storage systems.

In fact, several mathematical models have been developed and used to simulate the physical and electrochemical processes taking place inside batteries to aid for understanding and battery design.

b. Battery models

For batteries, different length scales can be simulated, depending on the simulator's needs, ranging from the atomistic (density functional theory) to pack level. (Figure 16)

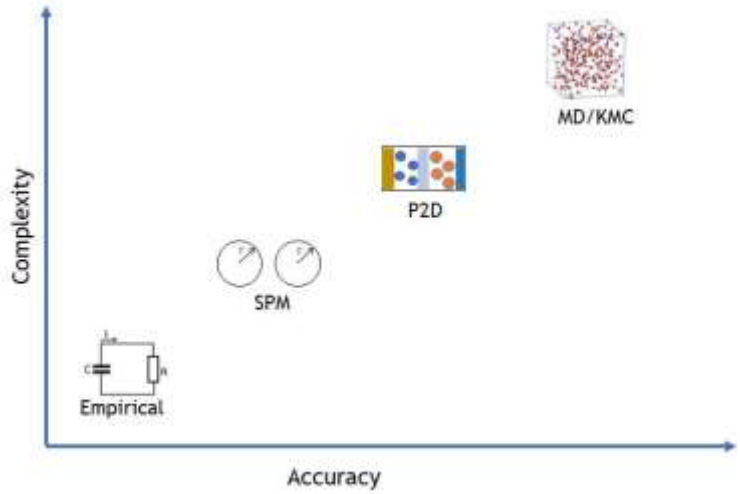

Figure 16: Representation of different battery models with respect to their complexity and accuracy

i. MD/KMC model

In terms of accuracy, at the molecular/atomic level, molecular dynamics simulations provide information on phenomena like the growth of a passivation film on the graphite electrode (SEI) for example. This simulation relies on the following principle: starting at any point, a molecular dynamics trajectory can explicitly track the movement of a molecule, using the forces provided by the Potential Energy Surfaces (PES) gradient.

Taking for example, the simulation of an adsorption process, the time scale of a vibrational event is close to a few picoseconds, orders of magnitude lower than the time scale of the migration between two adsorption sites (microseconds), which in that case represents the event of interest or rare event.

Given the number of events to simulate at that scale level, a Kinetic Monte Carlo (KMC) approximation is adopted, to focus on the rare event dynamics. The central idea behind this approximation is coarse-graining the time evolution to the discrete rare events. Also, KMC uses first principle electronic structure calculation.

ii. P2D model

The Pseudo 2D Model (P2D) takes into account migration phenomena in the electrolyte (mass transport) and the electrodes (diffusion), as well as kinetics phenomena in the electrodes, represented by partial differential equations (PDE). The resolution of these equations is usually carried out using Finite Element Analysis (FEA).

The P2D model is currently one of the most popular models to represent Li-ion batteries. Developed from the 1975 work from Newman and Tiedemann, the model is based on the porous electrode and the concentrated solution theory. [26]. The model assumes the porous electrode to be made of equally sized, isotropic, homogeneous spherical particles. The homogeneous description of the electrode microstructure results in a uniform simulated intercalation/deintercalation of lithium ions in the electrodes. This description has proven to give good results at low to moderate discharge/charge rates.

The *Batteries & Fuel Cells* module from the Comsol Multiphysics software (popular software for batteries-related numerical simulation) uses this approach. More specifically for lithium-ion batteries, the P2D model is referred to as “Dual-foil”. This P2D model considers as coordinates, an X one perpendicular to the materials’ sandwich and a radial dimension *r* within the active material particles assumed to be spherical and isotropic. This model is based on the porous electrode theory, which means that solid and liquid phases in each of the sandwich’s layer are treated as continuum and are characterized by their volume fraction within the layer and their surface area in contact with the other phases. Their physical properties (such as conductivity) are averaged over a volume element, small compared to the whole system size, but large compared to the pore’s size.[27]

iii. Empirical models

Empirical models appear to be the simplest, but also the least accurate ones. In order to be built, linear, polynomial, exponential and other functions or a combination of those are used to best approach experimental data. The determined parameters become constitutive of the built model.

The simplicity of the models allows for fast computation and makes them quite useful when envisioning battery management systems (BMS), for example.

However, their prediction capability is poor, as they showcase domain-specific strengths that limit their utility outside the envisioned environment.

iv. Single-Particle Model

In the single particle model, the whole electrode is viewed as a single particle. Similarly to the P2D model, this one incorporates the migration phenomenon that takes place in the electrolyte, as well as the kinetics phenomena at the electrodes using PDE. The resolution is often carried out using finite element analysis (FEA).

The surface area of the single particle representing the electrode is the same as the electrode. A difference from the P2D model resides in the fact that no variance in the solution phase is considered. However, diffusion and insertion kinetics are taken into account.

The Single-Particle model is usually used to simulate thin electrodes, used in low-current conditions.

v. Global Battery modeling

As electrochemical devices are subject to sometimes complex reactions, batteries also showcase thermal activity. As part of global efforts to predict batteries' behavior, this thermal component needs also to be simulated. Thermal models for batteries are usually realized using a battery 3D model, because geometry and surface area play an important role in heat transfer.

As a result, attempts were made to build thermo-electrochemical battery models presenting a P2D electrochemical model coupled to a 3D thermal model. [28] In this study, however, the thermal aspect will not be taken into account.

III. Mathematical model

1) Introduction to the model and simulation

As mentioned before, in order to capture the linear degradation and superlinear degradation, SEI growth and lithium plating were considered for modeling.

To accurately represent the studied chemistry, a P2D ageing electrochemical model is proposed for a cell containing graphite as an anode and LFP as its cathode. This model was based on a Newman model, developed in the early 90s by John Newman and then applied in different works [29]. For capacity loss, SEI growth was considered the most impactful phenomenon during the linear degradation phase and was therefore implemented in the model. Then, based on the work of Atalay et al. [30], and Yang et al.[36], the choice was made, to represent the superlinear degradation profile, to incorporate lithium-plating as well. A schematic of a cell is provided Figure 17.

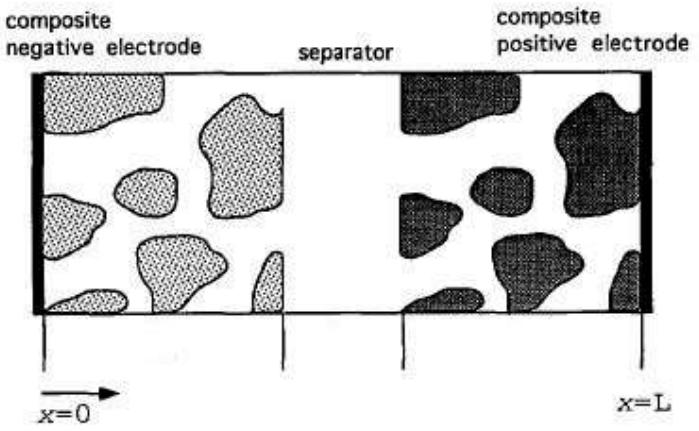

Figure 17 : Simplified scheme of the cell with the x-axis coordinates and the different cell components [33]

Along with cell thickness, the electrochemical system was modelled considering three subdomains, representing, respectively, graphite anode, separator, and LFP cathode. To describe the behavior of the concentration levels in the battery, the concentrated solution theory was used, as the electrolyte is composed of a binary lithium salt ($LiPF_6$) and a single-phase liquid solvent (in this case, 3:7 EC:EMC). Figure 18 shows the obtained cell view.

Figure 18 : Subdomains for the modeled cell

2) Newman's model

In the electrolyte-separator domain, the model solves for current conservation (Eq. 8) and mass conservation (Eq. 9), in which i_l is the ionic current density flowing in the liquid phase (electrolyte), σ_l denotes the electrolyte conductivity, f is the activity coefficient for the salt, t_+ is the transport number for Li^+, also called transference number, Φ_l is the electrolyte potential, c_l is the electrolyte salt concentration, ε_l is the electrolyte volume fraction and D_l is the salt diffusivity in the electrolyte. T, F and R are, respectively, the temperature, Faraday's constant, and the universal gas constant.

$$i_l = -\sigma_l . \nabla \Phi_l + \frac{2.\sigma_l . R.T}{F}\left(1 + \frac{\partial lnf}{\partial lnc_l}\right).(1 - t_+).\nabla lnc_l \quad (8)$$

$$\varepsilon_l \frac{\partial c_l}{\partial t} = \nabla(\varepsilon_l D_l \nabla c_l) - \nabla\left(\frac{i_l . t_+}{F}\right) + \frac{\nabla i_l}{F} \quad (9)$$

In Eq. 8, the term $-\sigma_l . \nabla \Phi_l$ is derived from Ohm's law applied to the ionic current in the electrolyte, whereas the term $\frac{2.\sigma_l . R.T}{F}\left(1 + \frac{\partial lnf}{\partial lnc_l}\right).(1 - t_+).\nabla lnc_l$ represents the concentration gradient present in the electrolytic solution. In Eq. 9, the term $\nabla(\varepsilon_l D_l \nabla c_l)$ is derived from the assumed equilibrium between anions and cations and $-\nabla\left(\frac{i_l . t_+}{F}\right) + \frac{\nabla i_l}{F}$ accounts for the transfer of charges.

In the electrodes, the current density is modelled by Equation 10,

$$i_s = -\sigma_s \nabla \Phi_s \quad (10)$$

where, Φ_s denotes the electric potential, and σ_s is the electrical conductivity.

Φ_l and c_l are defined in the electrolyte and the pore electrolyte. Assuming electroneutrality, c_l equally designates the Li^+(cations) and the An^- (anions) concentration.

a. Porous electrode theory

Within the Newman model, the porous electrode theory assumes that electrode particles are spherical, and that the electrode presents a homogeneous structure. The reaction occurs on the particle surface and lithium diffuses to and from the surface of the particles. The model solves the Fick law (Eq.11) for the diffusion of lithium ions,

$$\frac{\partial c_s}{\partial t} = -\nabla.(-D_s \nabla c_s) \quad (11)$$

with the following boundary conditions in Eq. 12 and Eq. 13,

$$\frac{\partial c_s}{\partial r} = 0\Big|_{r=0} \quad (12)$$

$$-D_s \frac{\partial c_s}{\partial r} = -\frac{\nabla i_s}{a_v F}\Big|_{r=r_p} \quad (13)$$

c_s is the concentration of Li in the solid phase. Fick law is solved locally, in a pseudo 1D dimension, and the solid phase concentration is calculated for the nodal points corresponding to the electrode discretization.

$\frac{\nabla i_s}{a_v F}$ represents the molar flux of lithium at the particle surface, caused by the insertion reactions. Furthermore, a_v represents the specific electrode surface area (Eq. 14) and is defined as,

$$a_v = \frac{N_{shape} \varepsilon_s}{r_p} \quad (14)$$

where N_{shape} is 1 for cartesian, 2 for cylindrical and 3 for spherical coordinates [31], ε_s is the active material volume fraction and r_p is the particle radius.

As the electrode is considered porous, pores and channels are present within. The paths leading to active material surface are not all equal and to be more representative of reality, path tortuosity has to be considered. Therefore, corrected values of diffusivity and conductivity are adopted, known as “effective” [32]. In this model, the Bruggeman relationship is considered, in which tortuosity is assumed to be a function of the material porosity. The effective diffusion coefficient $D_{l,eff}$, the effective liquid phase conductivity $\sigma_{l,eff}$ and the effective conductivity of the solid phase $\sigma_{s,eff}$ are expressed by Eq. 15,

$$\begin{cases} D_{l,eff} = \dfrac{\varepsilon}{\tau_{l,Brug}} D_l \\ \sigma_{l,eff} = \dfrac{\varepsilon}{\tau_{l,Brug}} \sigma_l \\ \sigma_{s,eff} = \dfrac{\varepsilon}{\tau_{l,Brug}} \sigma_s \end{cases} \quad (15)$$

The Bruggeman relation expresses the tortuosity factor (Eq. 16) as,

$$\tau_{l,Brug} = \varepsilon^{-0,5} \quad (16)$$

where $\tau_{l,Brug}$ and ε represent respectively the tortuosity and the porosity of the given material.

Therefore Eq. 17 is obtained,

$$\begin{cases} D_{l,eff} = \varepsilon^{1,5} D_l \\ \sigma_{l,eff} = \varepsilon^{1,5} \sigma_l \\ \sigma_{s,eff} = \varepsilon^{1,5} \sigma_s \end{cases} \quad (17)$$

b. Current densities and reactions

Regarding the reactions taking place at the anode and the cathode, the general expression for the total current density (Eq. 18) is as follows,

$$i_{tot} = \sum_m a_{v,m}.i_{loc,m} \quad (18)$$

where m represents the number of reactions taking place at the mentioned electrode, while $i_{loc,m}$ represents the current density generated by the m^{th} reaction.

Regarding the intercalation/deintercalation process of lithium ions within the active material, chemical kinetics are described by the Butler-Volmer equation (Eq. 19). In this particular case, the equation linked to the intercalation phenomenon

$$i_{int} = i_0 \left[exp\left(\frac{\alpha_a F \eta}{RT}\right) - exp\left(\frac{-\alpha_c F \eta}{RT}\right) \right] \quad (19)$$

where i_0 is the reference exchange current density of lithium intercalation, α_a and α_c are the anodic and cathodic charge transfer coefficients usually set to 0.5, assuming $\alpha_a + \alpha_c = 1$. [33]

The overpotential η due to the electrochemical reaction can be expressed in Eq. 20, where E_{eq} represents the open circuit potential (related to the SoC), here the equilibrium potential for the lithium intercalation reaction:

$$\eta = \Phi_s - \Phi_l - E_{eq} \quad (20)$$

c. Ageing implementation

i. SEI layer

To implement the linear degradation behavior attributed to SEI growth into the model, an approach similar to Kindermann et al. [34] is used. This work supposes that the SEI layer showcases maximum conductivity for lithium ions and poor conductivity for electrons. As such, the SEI layer is formed directly at the contact of graphite particles. Therefore, Eq. 20 needs to be modified (Eq. 21) and take into account an ohmic drop due to the SEI forming reaction:

$$\eta_{SEI} = \Phi_s - \Phi_l - E_{eq,SEI} - i_{SEI}.R_{SEI} \quad (21)$$

In this expression of the SEI-linked overpotential, $E_{eq,SEI}$ represents the SEI formation equilibrium potential, arbitrarily set to 0V in this work. R_{SEI} is calculated in Eq. 22,

$$R_{SEI} = \frac{\delta_{0,SEI} + \Delta\delta_{SEI}}{\sigma_{SEI}} \quad (22)$$

where $\delta_{0,SEI}$ represents the SEI initial thickness, $\Delta\delta_{SEI}$ the film's thickness increase and σ_{SEI} the electric conductivity. As the studied cells are commercial, subjected to formation cycling by the manufacturer to create SEI and ensure cell's stability, a value of $1\ nm$ was hypothesized for $\delta_{0,SEI}$.[34]

Following the work of Safari et al. [35] and Yang et al. [36], the model considers that the rate of SEI formation reaction presents two contributions. One is from the diffusion rate of EC (electrolyte solvent molecules) across the already formed SEI layer, and the second is from the surface kinetics.

To take into account these two phenomena, one must consider both the following Tafel equation (Eq. 23), about the surface kinetics,

$$i_{SEI} = -F.k_{0,SEI}.c_{EC,s}exp\left(-\frac{\alpha_{c,SEI}.F.\eta_{SEI}}{RT}\right) \quad (23)$$

And the mass conservation of EC (Eq. 24), given by,

$$-D_{EC}a_v\frac{c_{EC,s} - c_{EC,0}}{\delta_{SEI}} = \frac{i_{SEI}}{F} \quad (24)$$

where D_{EC} is the diffusivity of EC, $c_{EC,0}$ is the concentration of EC in the bulk electrolyte, and δ_{SEI} is the thickness of the SEI layer. If the left part of the equation represents the diffusive flux of EC across the SEI layer, the right part represents the consumption rate of EC through the SEI formation reaction.

The combination of those two contributions gives the following current density (Eq. 25) for the formation and growth of the SEI layer,

$$i_{SEI} = -\frac{F.k_{0,SEI}.c_{0,EC}}{exp\left(\frac{\alpha_{c,SEI}.F.\eta_{SEI}}{RT}\right) - \frac{k_{0,SEI}.\delta_{SEI}}{D_{EC}}} \quad (25)$$

Due to the formation and growth of the SEI layer, the anode local overpotential can be rewritten in Eq. 26,

$$\eta = \Phi_s - \Phi_l - E_{eq} - i_{tot}.R_{film} \quad (26)$$

where i_{tot} is total current density, sum of the different reactions taking place at the anode. While the SEI layer is forming, the total current density can be expressed by Eq. 27,

$$i_{tot} = i_{int} + i_{SEI} \quad (27)$$

and R_{film} is the resistance of the film covering the anode particles, which in that case is only due to the SEI layer.

When the anode local potential becomes negative vs $Li^+/Li(s)$, lithium plating would occur.

ii. Lithium plating

Based on the work of Yang et al. [39], the following current density (Eq. 28) for the formation of growth of lithium plating was adopted,

$$i_{lip} = -i_{0,lip} exp\left(\frac{-\alpha_{lip}.F.\eta_{lip}}{RT}\right) \quad (28)$$

where $i_{0,lip}$ represents the exchange current density of lithium metal deposition, α_{lip} is the cathodic reaction coefficient for lithium plating, arbitrarily set to 0.5, and η_{lip} corresponds to the lithium plating associated overpotential.

3) Model input

In the following part, essential battery structural input data is presented. For a model under Comsol Multiphysics to give an appropriate representation of reality, this data must be considered.

a. Geometrical attributes

The first parameters as input in the Newman model are the geometrical ones, for the electrodes and the separator, such as the electrodes' and separator's thickness or the electrode material particle size. This data can be obtained thanks to measurements done in a lab prior to the elaboration of the numerical model. The mass of the electrodes should also be measured.

b. Electrode composition

i. Porosity-Volume fractions

As the cell's geometrical parameters intervene in the calculation of the different material mass and volume fractions, they have to be known. The volume fractions intervenes in different equations of the Newman model and as this data is usually not provided by the manufacturer, it needs to be calculated in order to have a representative model.

From these data, and based on the work of Chen et al. [37], the following formulas should be used to estimate the solid volume fraction (Eq. 29) and the liquid volume fraction (Eq.30),

$$\varepsilon_s = \frac{M_{coat.}}{L_{electrode} \times \rho_{electrode}} \quad (29)$$

$$\varepsilon_l = 1 - \varepsilon_s \quad (30)$$

where $M_{coat.}$ designates the mass of the electrode (only one graphite or LFP layer), $L_{electrode}$ is the thickness of the electrode, and $\rho_{electrode}$ is the density of the electrode.

In this case, the term $\rho_{material}$ (Eq.31) was calculated as a weighted sum of $\rho_{active\ material}$ and $\rho_{binders}$ so that,

$$\rho_{electrode} = \varepsilon_{active\ material} \cdot \rho_{active\ material} + \varepsilon_{carbon\ binder} \cdot \rho_{carbon} + \varepsilon_{polymer\ binder} \cdot \rho_{polymer} \quad (31)$$

in order to take into account the solid volume contribution from the inactive material to the total solid volume fraction of the electrode.

Though electrodes, such as graphite, can be subjected to volume change during battery operation, these solid volume fractions are assumed to be constant throughout the simulation.

ii. Active sites concentration

The active sites concentration $c_{s,max}$, which represents the maximum lithium hosting capacity expressed in $mol.m^{-3}$, is an important parameter for the estimation of the initial battery capacity. As a matter of fact, the initial capacity of an electrode in the Comsol software is estimated in Eq.32,

$$Q_{electrode} = c_{s,max}.\varepsilon_s.L_{electrode}.F.A_{electrode} \quad (32)$$

where $A_{electrode}$ represents the electrode surface area.

Though a value of $c_{s,max}$ is given for each electrode material in many softwares, using geometrical data and material density can be useful to correctly determine the $c_{s,max}$ value, as this value can vary from one manufacturer to another according to the electrode manufacturing process.

The capacity (Eq. 33) of the anode and the cathode can then be calculated as follows,

$$Q_{electrode} = m_{electrode}.q_{electrode} \quad (33)$$

with $m_{electrode}$ being the mass of the electrode, and $q_{electrode}$ being the mass capacity of the material, coming either from available lab results or literature-based assumptions.

For a given electrode and therefore a given active material (graphite or LFP), the maximum lithium hosting capacity $c_{s,max}$ is expressed by Eq. 34,

$$c_{s,max} = \frac{m_{electrode}.q_{electrode}}{\varepsilon_s.L_{electrode}.F.A_{electrode}} \quad (34)$$

iii. Electrode balancing

Battery manufacturers want to optimize their battery design by reducing the weight of their battery, therefore carefully choosing the quantity of materials they put in the battery. However, some electrochemical constraints bind the materials quantity together, particularly for the active material, in our case graphite and LFP.

Though no parasitic reactions were considered in the model for the LFP cathode, they exist. For example, full delithiation of the cathode can be detrimental to the host matrix and could destroy it. Furthermore high potentials could cause irreversible electrolyte oxidation (CEI) or dissolution of metal ions from the lithium oxide matrix. Therefore, engineers select a maximum electrode voltage. This voltage implies a limitation on the positive electrode lithiation window, which in turn means that more active material than the nominal cell capacity has to be used.

Therefore, electrode balancing (choosing the right amount of anode material) cannot be based solely on the nominal cell capacity, as some of the cathode host capacity might not be used.

iii.1. Anode/Cathode ratio (N/P ratio)

When the battery is at the end of the charging process, the anode potential drops as it gets filled with lithium ions. As previously seen in the description of ageing mechanisms, low potentials can reveal themselves to be harmful to the anode, as they can accelerate the SEI formation reaction rate, and can tend to the potential for lithium-plating. As a result, to avoid full lithiation, it is common to add an excess amount of negative electrode material to avoid those low potentials and increase the battery lifetime. This excess amount of negative electrode material is often visible in the defined $\frac{Anode}{Cathode} ratio$ also referred to as the N/P ratio given by Eq. 35,

$$N/P\ ratio = \frac{Q_{anode}}{Q_{cathode}} \quad (35)$$

iii.2. Shift of operational window

Before calculating the N/P ratio, it is important to introduce the Shift of Operational Window factor (SOW). This factor will be further described after presenting the electrode potential.

To correctly characterize a cell, and appropriately initialize a simulation model, knowing the electrode materials potential window is very important, as part of the electrode balancing procedure.

To know these potentials, an incremental capacity analysis (ICA) is necessary. This technique must be applied on both half-cells, one with the positive electrode material and the other with the negative electrode material. The following curves, on Figures 19 and 20, represent the evolution of the electrode potential with respect to the amount of lithium stored within (electrode SoC), in percentage.

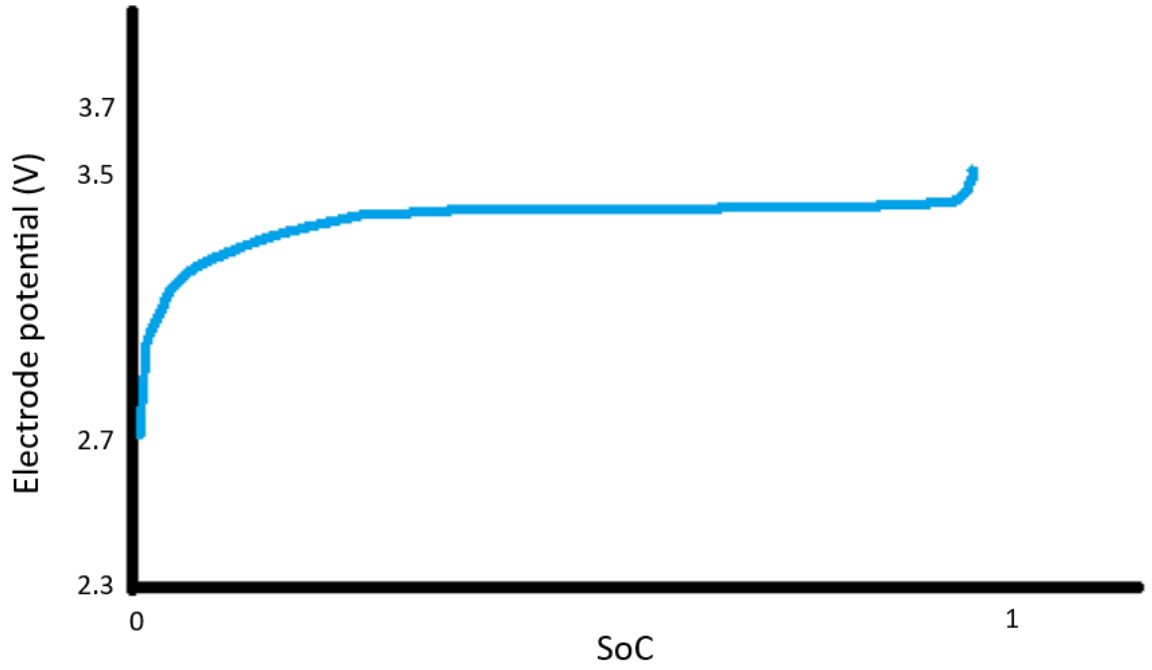

Figure 19: Equilibrium potential evolution for Graphite anode versus SoC

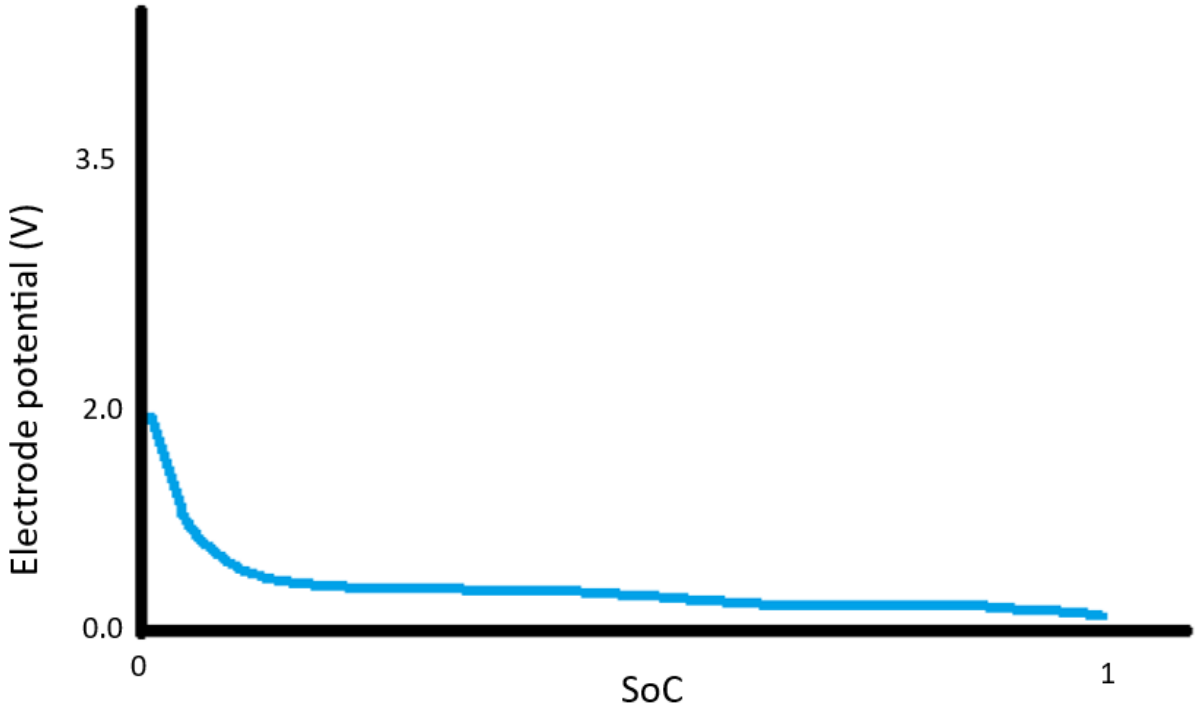

Figure 20: Equilibrium potential evolution for LFP cathode versus SoC

These two graphs show the pseudo-Open-Circuit Potential (pseudo-OCP) that can be obtained for a graphite and an LFP electrode. The pseudo-OCPs are represented versus the state of charge going from 0% lithiation to 100% lithiation.

The effect of the first cell formation cycles is shown below taking one cycle as an example. At the beginning, Fig. 21.a the cathode is fully lithiated and the anode is completely delithiated. During the first charge, a part of the electrons and is involved with parasitic reactions such as SEI formation, depleting the cyclable lithium stock. This provokes a shift of the anode potential curve towards the left (Fig. 21.b), with the shift size proportional to the quantity of consumed lithium and electrons in the side reaction. The resulting capacity is indicated at Fig.21.c.

This means that when the battery is being sold, the manufacturer has already performed the first cycles, known as “formation cycles”. Upon reception, the commercial cell therefore already presents this shift, proof of the depletion of the initial cyclable lithium stock.

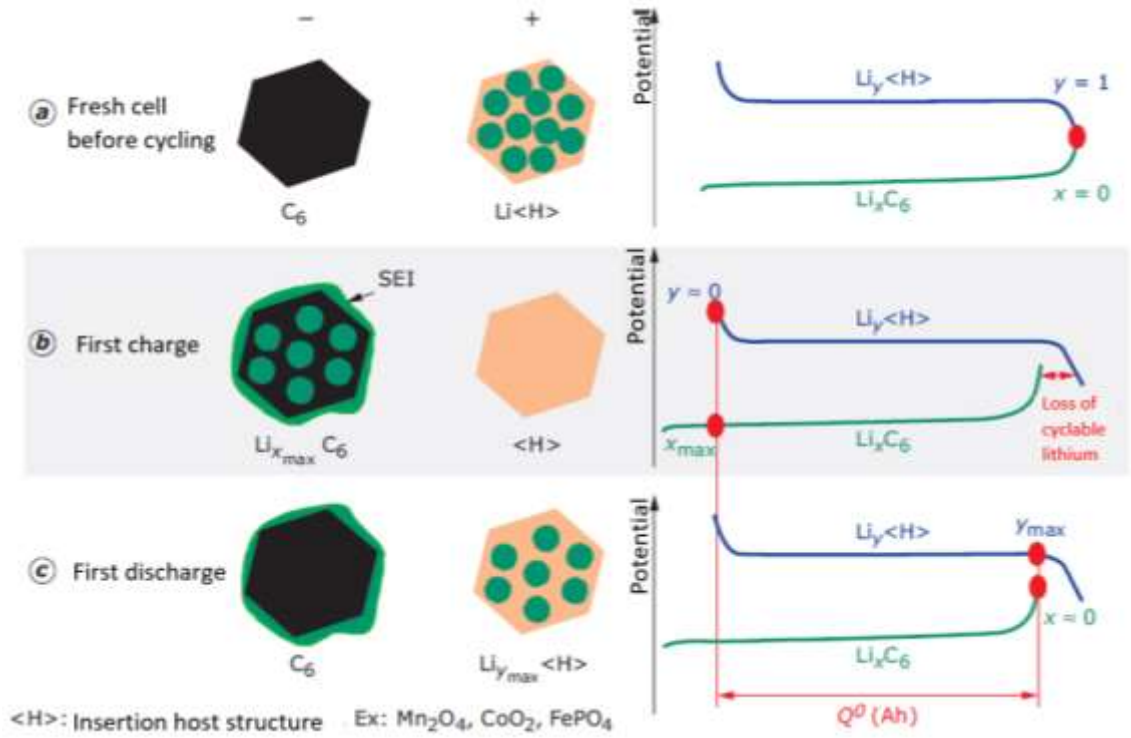

Figure 21: Illustration of the effect of first cycles on the electrodes potential window in the assembled cell [42]

This shift, result of the loss of cyclable lithium on Figure 21.b, called shift of operational window corresponds to the shift of operational window and needs to be incorporated into the model for appropriate electrode balancing.

The approach used in the porosity calculation and the active sites concentration calculation allowed to find a N/P ratio equal to the 1,2 value provided by the lab.

$$N/P\ ratio = \frac{Q_{anode}}{Q_{cathode}.(1 - SOW)} = 1{,}2 \quad (36)$$

This parameter is often an input for several electrochemical models. For example, in the Comsol software, it is included in the “Initial cell charge distribution section” from the Li-ion library, as the fraction of hosted capacity excess in negative electrode. (Figure 22)

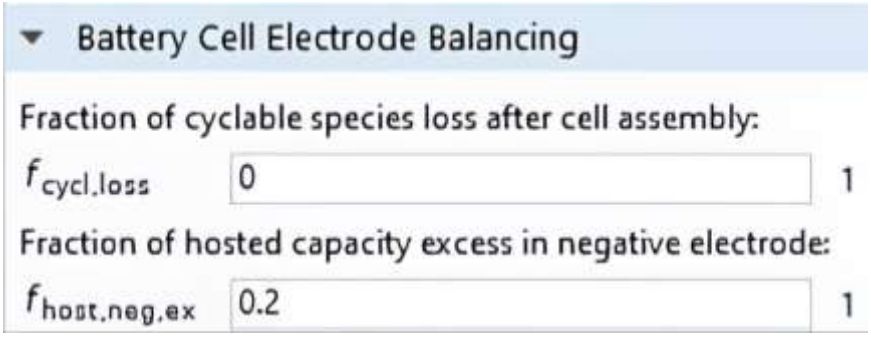

Figure 22: Initial cell charge distribution COMSOL section

iv. Time accelerating factor

Usually, a battery would need several cycles to show any noticeable capacity fade, and the cycle-to-cycle capacity fade can be assumed to be small.

Every simulated charge-discharge cycle can be the result of an averaged ageing behavior, assuming that for one charge-discharge cycle, all the lithium captured in the SEI layer is stemming from the graphite anode. With this assumption, the capacity loss can be accelerated, rewriting the SEI forming reaction equation (Eq.37) with,

$$(\tau - 1)S + (\tau - 1)Li(s) \rightarrow (\tau - 1)P_{SEI} \quad (37)$$

and knowing that the elementary reaction is given by Eq. 38,

$$S + Li^{+} + e^{+} \rightarrow P_{SEI} \quad (38)$$

The overall reaction results in Eq. 39,

$$\tau S + Li^{+} + e^{-} + (\tau - 1)Li(s) \rightarrow \tau P_{SEI} \quad (39)$$

Here, τ can be seen as a time acceleration factor. This term represents how many real cycles each simulated battery cycle would represent. [31]

v. Battery operation parameters

It is important to set the battery operation parameters right in the model, in order to have a good comparison with experimental data. This can include the Depth-of-Discharge (DoD), the C-rate, in charge and discharge, the operating temperature. If a model description was given above, it is important to keep in mind that in reality, many battery ageing factors are interconnected and interdependent. This is the reason why one needs the most thorough description of its input data in order to obtain reliable results, or at least the most reliable results.

4) Exploitation of experimental data

a. Cycling trials data

The data provided by the lab consisted in discharge capacity data for a Gr/LFP cell. The cell was subjected to cycling in order to register the cell's capacity at different moments in time and after a certain number of cycles.

In order to register the capacity, a charge at C/5 was performed followed by a discharge at C/5.

The choice of C-rate is motivated by the fact that a high current doesn't allow the lithium ions to properly explore all the active sites in the electrodes during whether a charge or a discharge sequence. Very low C-rates are usually employed to precisely approach equilibrium potentials function of the state of lithiation for a given electrode. In the current case however, as the objective is to approach the battery discharge capacity, a low C-rate of a value of C/5 is sufficient. During the discharge phase of the investigation, the integral of the current over the discharge time gives the battery capacity.

The graph obtained for a tested cell is presented in Figure 23.

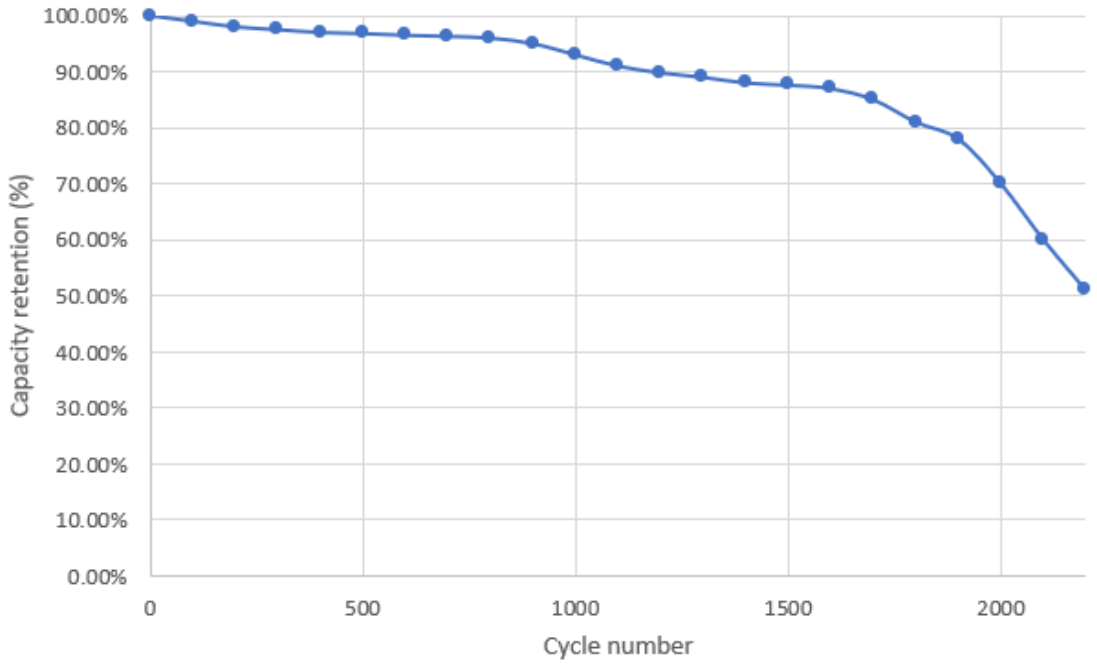

Figure 23: Gr/LFP cell ageing profile, showing capacity retention through cycling

b. SEI layer formation and growth simulation

Considering that prior to 1800 cycles, the ageing is linear and that after, the ageing becomes superlinear, it is possible to extract a capacity decrease rate, at least in the linear part (Fig.24).

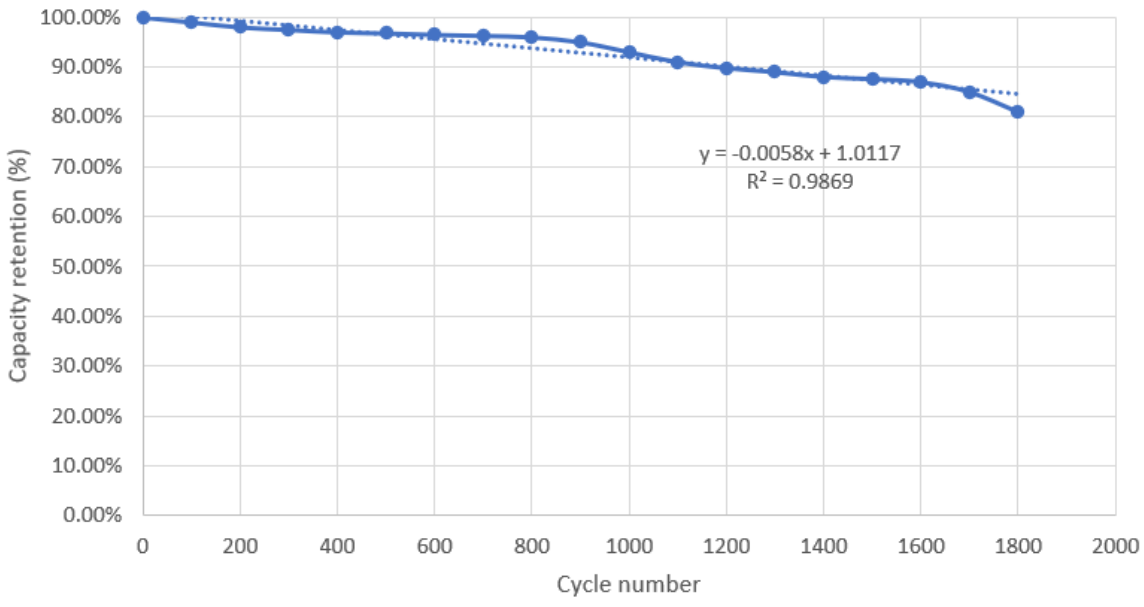

Figure 24: Linear degradation part, with linear regression

The obtained experimental degradation rate for the linear ageing part of the capacity evolution had the following value, referred to as r, $r = -0.0058$.

To verify if the COMSOL model was adequately calibrated regarding, firstly, the linear degradation part, choice was made to represent the capacity drop obtained in Comsol. As the formation and growth of the SEI layer was considered to be the only responsible phenomenon for the linear capacity decrease, it was the only simulated phenomenon in the following graph, Figure 25.

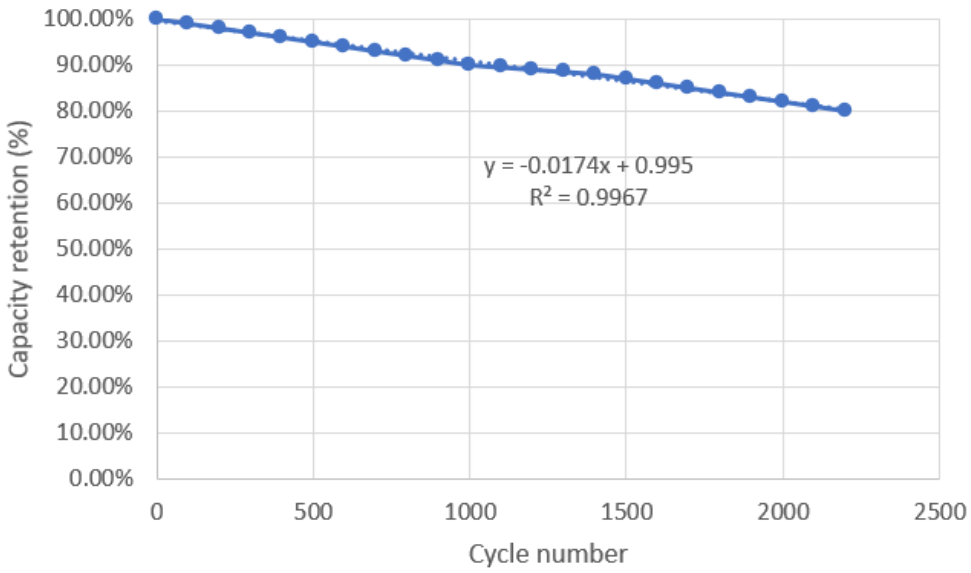

Figure 25: Capacity retention evolution in COMSOL for the SEI layer

The defined ratio between the two decrease rates is the following:

$$\gamma = \frac{r_{experience}}{r_{modeling}} \quad (37)$$

The ratio is equal to: $\gamma = \frac{0.0058}{0.0174} = 0.33$.

As expected, the multiplication by γ of the SEI formation current density i_{SEI}, provides a capacity retention evolution (Fig. 26) close to the real one.

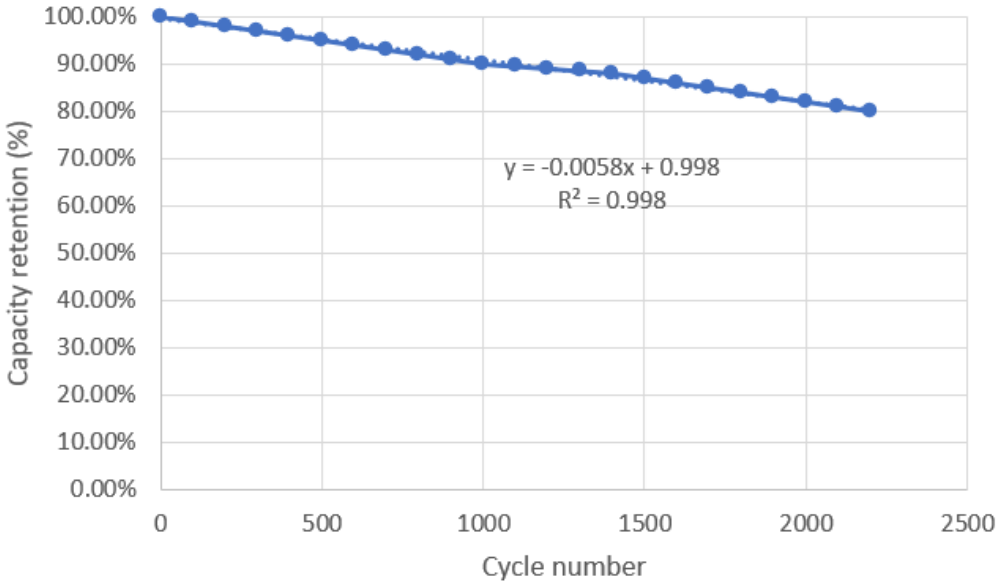

Figure 26: Comsol capacity fade with corrected SEI current density

Though this first manipulation does not highlight which specific term in the SEI forming equation should be modified in order to provide an experiment-like behavior, the correction by the γ factor still allows the model to be representative of the experiment for the linear degradation part.

c. Lithium plating and superlinear degradation

A great deal of writing has been devoted to the presentation of the attempt of calibration for the SEI layer, the linear degradation part of the cell ageing profile. This is due to the fact that simulation of the superlinear part (Fig. 27) has only given partial results.

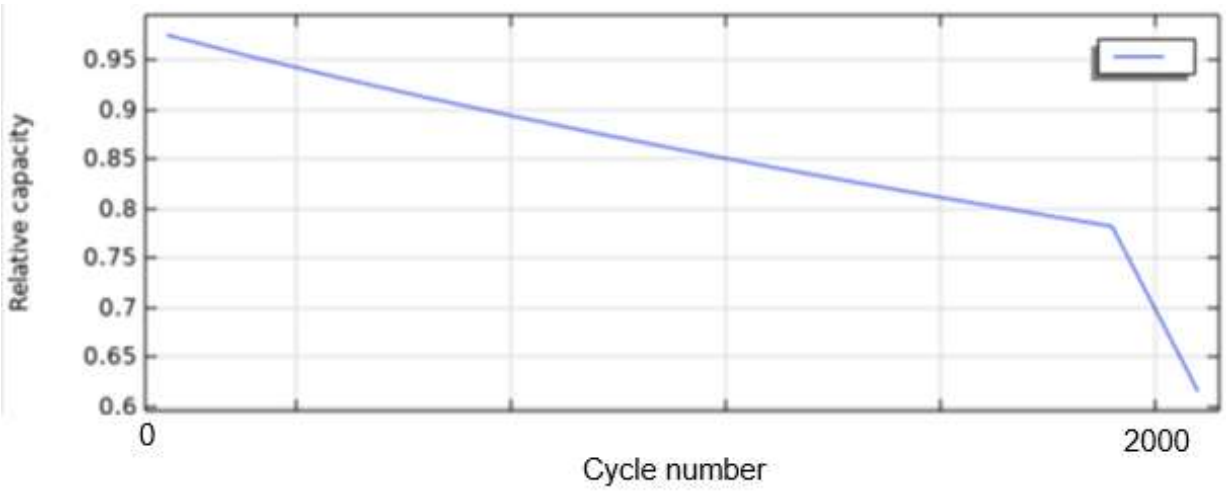

Figure 27: Knee-point phenomenon observed for the simulated Gr/LFP cell

Though comforting, this first result observable for capacity, is not fully conclusive as it is suspected that the observed knee-point could be a side effect from the local electrolyte depletion (Fig. 28).

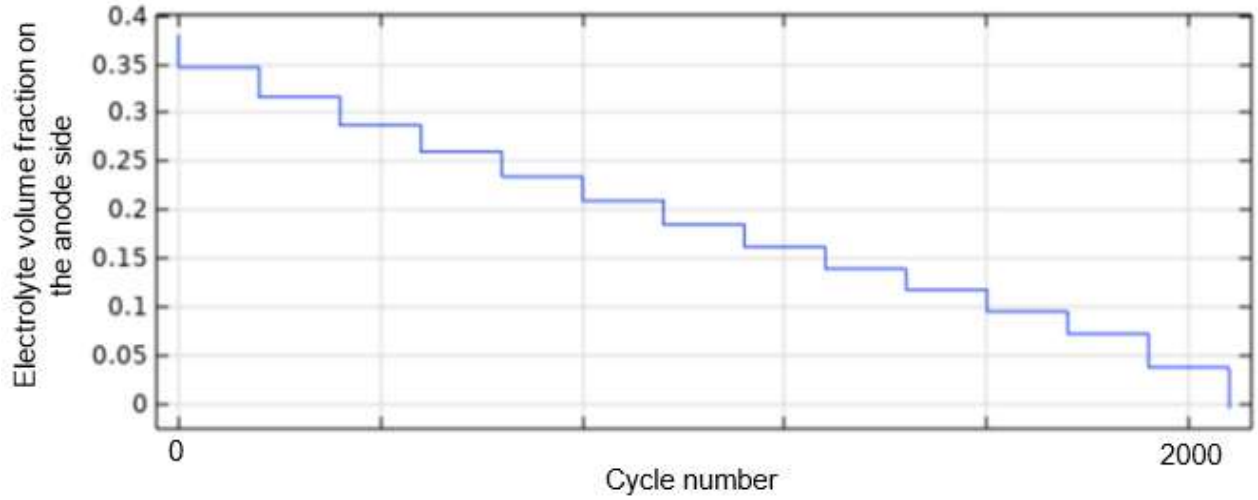

Figure 28: Electrolyte volume fraction evolution versus the number of cycles

Indeed, it has been observed in Comsol, that, by de-activating the option reducing the electrolyte volume fraction, the knee-point phenomenon does not appear and the lithium plating reaction is not observed. Though porosity seems to play an undoubtable role in the surface kinetics equation, its role is still unclear in its apparent influence on global overpotential and appearance of lithium-plating.

Conclusion

The adequate choice of an electrochemical device for energy storage needs to undergo scrutiny. The knowledge of materials and physico-chemical phenomena at play is key to understand a system's behavior and as seen in this study, a system's behavior through time. Once known, different equations need to be attributed to different phenomena in order to be able to build a computer model that would allow one to perform simulations. Provided a model's robustness, these simulations aim at forecasting the behavior of a battery and therefore choose the appropriate one for the adequate application and use.

During this project, an attempt was made to describe the ageing of a Gr/LFP cell, taking into account two degradation phenomena, respectively SEI layer formation, growth and lithium-plating.

While the calibration of Newman's model needs to consider several battery operating parameters and structural characteristics, taking into account the SEI layer formation, work still needs to be done to be sure of the simulation results coherence with real cell trials.

The objective of correctly simulating the metallic lithium deposition and the related knee-point has been reached by several research teams. However work still needs to be done, regarding the quantification of uncertainties and the better calibration of model parameters, to build more robust models, able to explore other operating configurations. Indeed, this work has not allowed to fully comprehend the causes for the appearance of the *knee-point* phenomenon.

A better calibration of the SEI layer formation and growth in the simulation, through not only the study of the capacity fade rate, but also of other linked variables such as the film resistance and the evaluation of uncertainties could help solving some issues and lead to an appropriate modelling of the cell and probably influence the outcome on the *knee-point* simulation.

References

[1]: M. Winter, R. J. Brodd (2004) What are batteries, fuel cells, and supercapacitors? *Chemical Reviews.* 104(10) p. 4245-4270

[2]: H. A. Kiehne (2003), Battery Technology Handbook

[3]: Ma et al. (2016), Surface and interface issues in spinel $LiNi_{0.5}Mn_{1.5}O_4$: insights into a potential cathode material for high energy density lithium-ion batteries, *Chemistry of Materials* 28(11)

[4]: S. Megahed, B. Scrosati (1994), Lithium-ion rechargeable batteries, *Journal of Power Sources*. 51(1-2) p.79-104

[5]: Zou et al. (2015). Combined State of Charge and State of Health estimation over lithium-ion battery cell cycle lifespan for electric vehicles, *Journal of Power Sources.* 273. p. 793-803

[6]: (2021) The pricing power at LFP producers increased with its cost-effectiveness on rising costs; SMM

[7]: Jeffrey W. Fergus (2010). Recent developments in cathode materials for lithium ion batteries. *Journal of Power Sources.* 195(4). P. 939-954

[8]: J.-M. Tarascon, M. Armand (2001) Issues and challenges facing rechargeable lithium batteries. *Nature.* 414, p. 359-367

[9]: P.U. Nzereogu et al. (2022). Anode materials for lithium-ion batteries: A review; *Applied Surface Science Advances.* 9

[10]: Matthew B. Pinson, Martin Z. Bazant (2013) Theory of SEI formation in rechargeable batteries: Capacity fade, Accelerated Aging and Lifetime prediction. *J. Electrochem. Soc.* 160(2) p.243-250

[12]: P. Zanello. (2003) Inorganic Electrochemistry: Theory, Practice, and Application. *Royal Society of Chemistry*

[11]: N. Nitta, F. Wu et al. (2015) Li-ion battery materials : present and future. *Materials Today.* 18(5) p.252-264

[12]: E. Peled, S. Menkin,(2017). Review-SEI: Past, Present and Future. *J. Electrochem. Soc.* 164

[13]: Jeffrey W. Fergus (2010). Ceramic and polymeric solid electrolytes for lithium-ion batteries. *Journal of Power Sources.* 195(15) p. 4554-4569

[14]: Toshio Matsushima (2009) Deterioration estimation of lithium-ion cells in direct current power supply systems and characteristics of 400-AH lithium-ion cells. *Journal of Power Sources.* 189(1) p. 847-854

[15]: Rutooj Deshpande et al. (2012) Battery cycle life prediction with coupled chemical degradation and fatigue mechanics. *J. Electrochem. Soc.* 159(10)

[16]: Xuebing Han et al. (2014) A comparative study of commercial lithium ion battery cycle life in electrical vehicle: Aging mechanism identification. *Journal of Power Sources*. 251, p. 38-54

[17]: Xuebing Han et al.(2019) A review on the key issues of the lithium ion battery degradation among the whole life cycle. *eTransportation*. 1

[18]: Zhe Li et al. (2014) A review of lithium deposition in lithium-ion and lithium metal secondary batteries. *Journal of Power Sources.* 254, p.168-182

[19]: Christoph R. Birkl, Matthew R. Roberts(2017). Degradation diagnostics for lithium ion cells. *Journal of Power Sources.* 341, p.373-386

[20]: K. Zaghib et al. (2011) Safe and fast-charging Li-ion battery with long shelf life for power applications. *Journal of Power Sources.* 196, p.3949-3954

[21]: Peter M. Attia et al.(2022) Review-« Knees » in Lithium-ion battery aging trajectories. *J. Electrochem. Soc.* 169(6)

[22]: Klein et al. (2021) Demonstrating apparently inconspicuous but sensitive impacts on the rollover failure of lithium-ion batteries at a high voltage. *ACS Applied materials & Interfaces.*

[23]: Languang Lu et al. (2013) A review on the key issues for lithium-ion battery management in electric vehicles. *Journal of Power Sources.* 226(3), p.272-288

[24]: Xianke Lin et al. (2021) Lithium plating mechanism, detection and mitigation in lithium-ion batteries. *Progress in Energy and Combustion Science.* 87

[25]: Mark F. Horstemeyer (2012) Using multiscale modeling to invigorate engineering design with science. *Integrated computational materials engineering (ICME) for metals.*

[26]: James Le Houx et al. (2020) Physics based modelling of porous lithium ion battery electrodes-A review. *Energy Reports.* 6(5) p.1-9

[27]: John Newman, Karen E. Thomas-Alyea (2004) Electrochemical Systems

[28]: Dafang Wang et al. (2022) An electrochemical-thermal model of lithium-ion battery and state-of-health estimation. *Journal of Energy Storage.* 47

[29]: Thomas F. Fuller, Marc Doyle, John Newman (1994) Simulation and Optimization of the dual lithium ion insertion cell. *J. Electrochem. Soc.* 141(1)

[30]: S. Atalay et al. (2020) Theory of battery ageing in a lithium-ion battery: Capacity fade, nonlinear ageing and lifetime prediction

[31]: *Theory for the Lithium-Ion Battery Interface*, Comsol Multiphysics documentation

[32]: Bernhard Tjaden et al. (2016) on the origin and application of the Bruggeman correlation for analysing transport phenomena in electrochemical systems. *Current Opinion in Chemical Engineering.* 12, p.44-51

[33]: C. Heubner et al. (2015) Investigation of charge transfer kinetics of Li-intercalation in LiFePO4. *Journal of Power Sources.* 288, p. 115-120

[34]: Frank M. Kindermann et al. (2017) A SEI modeling approach distinguishing between capacity and power fade. *J. Electrochem. Soc.* 164

[35]: M. Safari, M. Morcrette, A. Teyssot, C. Delacourt (2008) Multimodal physics-based aging model for life prediction of Li-ion batteries. *J. Electrochem. Soc.* 156

[36]: Xiao-Guang Yang et al. (2017) Modeling of lithium plating induced aging of lithium-ion batteries: transition from linear to nonlinear aging. *Journal of Power Sources.* 360, p.28-40

[37]: Chang-Hui Chen et al. (2020) Development of experimental techniques for parameterization of multi-scale lithium-ion battery models. *J. Electrochem. Soc.* 167(8)

[38]: Solomon T. Oyakhire et al. (2022) Electrical resistance of the current collector controls lithium morphology. *Nature Communications.* 13

[39]: Ruoyu Xiong et al. (2023) Overpotential decomposition enabled decoupling of complex kinetic processes in battery electrodes. *Journal of Power Sources.* 553

[40]: Michael A. Roscher et al. (2009) Characterisation of charge and discharge behaviour of lithium ion batteries with olivine based cathode active material. *Journal of Power Sources.* 191(2), p.582-590

[41]: K. Smith et al. (2006) Solid-state diffusion limitations on pulse operation of a lithium ion cell for hybrid electric vehicles. *Journal of Power Sources.* 161(1), p.628-639

[42]: C. Delacourt et al. (2014) Vieillissement des accumulateurs lithium-ion dans l'automobile. *Techniques de l'Ingénieur*

[43] : V. Satopää et al. (2011) Finding a Kneedle in a Haystack: detecting Knee-Points in System Behavior. *IEEE*